Investigation into the Material Response of Concretes when Subject to Blast and Fragment Loading

Phillip Mellen

School of Civil, Environmental, and Mining Engineering
University of Adelaide

June 2019

Abstract

Vehicle Bourne Improvised Explosive Devices (VBIEDs) are utilised globally by terrorist organisations and radical individuals to inflict mass casualties. Many of these casualties are caused by the collapse of structures due to damage sustained by the blast and fragmentation loadings produced by the VBIED. As such it is important to understand how these loadings affect structures so as to improve design and increase structure survivability.

Historically significant research effort has been invested in understanding the blast and fragmentation loadings produced by conventional weapons. The loadings produced by VBIEDs are often considerably different with much larger, slower fragments. Little work has been undertaken in documenting these loadings and how they damage structural materials such as concrete. As such, when designing for threats of this type the fragmentation loading produced by a VBIED is often ignored.

This thesis aims to investigate; the loadings produced by bare explosive charges and VBIED surrogate charges, and how the blast and fragmentation loadings contribute to the deflection and damage of concrete panels. Panels with approximate dimensions of 1200 mm by 1200 mm and with thicknesses varying between 100 and 200 mm were tested. Panels were constructed from low-strength concrete, moderate-strength concrete, and Ultra-High Performance Concrete (UHPC).

Testing found that the fragment loading produced by the VBIED surrogate was sufficient to produce a global response in the panels as well as localised damage. As such, fragmentation loadings should not be ignored when predicting the response of structures to VBIED threats. Synergistic effects, between the blast and fragmentation loadings were, were observed for panels with sufficiently low flexural stiffness.

Declaration

I certify that this work contains no material which has been accepted for the award of any other degree or diploma in my name, in any university or other tertiary institution and, to the best of my knowledge and belief, contains no material previously published or written by another person, except where due reference has been made in the text. In addition, I certify that no part of this work will, in the future, be used in a submission in my name, for any other degree or diploma in any university or other tertiary institution without the prior approval of the University of Adelaide and where applicable, any partner institution responsible for the joint-award of this degree. I acknowledge that copyright of published works contained within this thesis resides with the copyright holder(s) of those works. I also give permission for the digital version of my thesis to be made available on the web, via the University's digital research repository, the Library Search and also through web search engines, unless permission has been granted by the University to restrict access for a period of time. I acknowledge the support I have received for my research through the provision of an Australian Government Research Training Program Scholarship.

Phillip Mellen

Acknowledgements

I would like to express my gratitude to my supervisors, Dr Terry Bennett and Dr Christine Shanahan (nee Pienaar), for their guidance through this entire process and steadfast support despite a number of challenges that have risen along the way. I would also like to thank the many staff members of both DST Group and the University of Adelaide who have assisted me in innumerable ways. In particular I would like to acknowledge the technical support provided by the staff of the Land Weapons Technology Group including, John Draper, Jared Freundt, Steve Stojko, and Mauro Carrabba. Without their help and expertise on the Pt Wakefield range, in less than optimal weather conditions, this work would not have been possible.

Contents

Included Publications

P. Mellen, C. Shanahan and T. Bennett, *Blast and fragmentation loading indicative of a VBIED surrogate for structural panel response analysis,* International Journal of Impact Engineering, vol. 126, pp. 172-184, 2019

1. Introduction

This Master's thesis will work towards building knowledge of the mechanisms by which Vehicle Bourne Improvised Explosive Devices (VBIEDs) load and damage structural elements. This initial chapter well provide the motivation for the research, a background and overview of work undertaken in this field, and the structure of the thesis document.

Background

Vehicle Borne Improvised Explosive Devices (VBIEDs) are a form of Improvised Explosive Device in which a car or other vehicle is loaded with explosives and then detonated. The explosive material may be commercially sourced explosive, home-made explosive, or repurposed military explosive. VBIEDs are an effective weapon as they are a low cost and inconspicuous way to transport a large amount of explosive material into close proximity of a target.

VBIED's are not a new technology with reports of a gunpowder laden carriage used in the attempted assassination of Napoleon in 1800. In more recent years these weapons have been widely used by terrorist groups and individuals. Some statistics for recent attacks resulting in considerable casualties are shown below in table 1.

Table 1: VBIEDs statistics from selected VBIED attacks since 1983

Date	Location	Deaths	Injuries
14th October 2017	Mogadishu, Somalia	587	316
15th April 2017	Aleppo, Syria	126	>55
13th July 2016	Baghdad, Iraq	323	225
7th August 1998	US Embassies, Nairobi, Kenya, and Tanzania	223	>4500
19th April 1995	Oklahoma City, USA	168	680
23rd October 1983	Lebanon, Beirut	241	75

In many of these attacks a large cause of casualties was not injury directly from the explosive blast or fragments generated by the VBIEDs, but due to the partial or complete collapse of structures that had been damaged by the VBIEDs. As such it is important for structural engineers to understand the loadings generated by VBIEDs in order to design structures that are more resilient to these types of loadings.

In Australia there have fortunately been no successful large scale VBIED attacks. Recent counter-terrorism arrests and prosecutions within Australia relating to plots involving IEDs and explosives demonstrate the ongoing risk domestically [1]. These threats remain a concern for Defence and National Security agencies as they work to maintain domestic security and safety of Australian deployed and strategic assets.

2. Literature Review

Blast Waves

When an explosion occurs a large amount of energy is deposited in a small volume. This produces an increase in pressure and flow that travels out from the explosion as a blast wave [2]. For air with an ambient pressure p_0, the blast wave will produce an instantaneous increase in pressure to an overpressure, P_s, followed by a rapid decrease in pressure. At a time, t^*, after the arrival of the blast wave, the pressure will drop below the ambient pressure before equalising back to the ambient pressure. An example of this general time history is shown below in figure 1. The time in which the pressure is greater than the ambient pressure is known as the positive phase, whilst the period during which the pressure is lower than the ambient pressure is known as the negative phase. Typically the positive phase imparts a much greater impulse than the negative phase. In the near field, close to the explosion, or if there are reflecting surfaces, the pressure history generated by the blast wave may be drastically different.

Pressure Approximations

The pressure history of a blast wave is often approximated or idealised in order to simplify problems.

Linear Pressure History

The simplest approximation for the pressure history is a simple triangular pressure history of the form [3]:

$$p(t) = p_0 + P_s\left(1 - \frac{t}{t^*}\right) \qquad 2.1$$

For many applications only concerned with the peak overpressure and the impulse of the positive phase this approximation is adequate, however it does not include the negative pressure phase.

Friedlander Equation

Perhaps the most popular idealised pressure history is the Friedlander equation. First noted by Friedlander in 1936 this equation was designed to give an accurate pressure history for blast in the free field. The equation is of the form [3]:

$$p(t) = p_0 + P_s e^{-\frac{t}{t^*}}\left(1 - \frac{t}{t^*}\right) \qquad 2.2$$

A diagram of the curve produced by the Friedlander Equation is shown below.

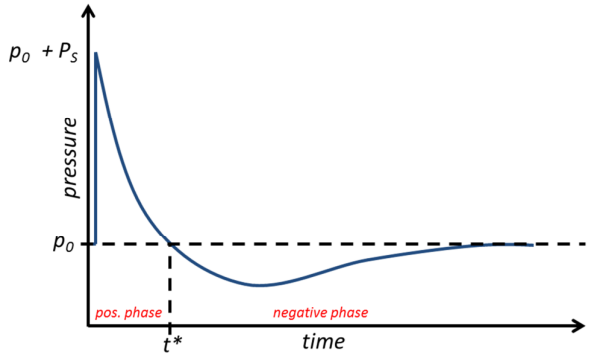

Figure 1: Diagram of Friedlander Equation showing pressure history of a blast wave

Fragmentation

When explosives are detonated within a container or casing the high pressure generated by the detonation breaks apart the container or casing generating fragments which are ejected with a high velocity in multiple directions. The shape, material and initial velocities of fragments can vary greatly and is dependent on the container or casing, and the explosive used. Conventional munitions such as grenades, bombs, torpedoes or missiles, generally produce relatively small, consistently sized, high velocity fragments from their metal casings, whilst IEDs can produce fragments from a wide variety of materials with huge variation in fragment size, velocity and distribution.

Gurney Model

When considering the loading of fragments on structures the two most important fragment properties are mass and velocity. The velocity at which an explosive will drive metal can be predicted using equations developed by R. W. Gurney [4]. These equations are based on the following assumptions:

- When an explosive detonates it produces a given amount of energy per unit mass of the explosive, which is converted into the kinetic energy of the driven metal and the gaseous detonation products.
- The gaseous detonation products have a uniform density and a linear velocity profile.

Whilst these assumptions seem to deviate significantly from actual gas dynamics, these deviations only affect the correlation at very large (>10) or low (<0.2) values of M/C (casing mass to explosive charge mass ratio) [5] . Whilst more comprehensive reviews of the Gurney method and the many formulas are available [6] only two are shown below. In these *E* is the *Gurney Energy*, a property of an explosive, and M/C is the driven metal to explosive charge mass ratio.

$$\textit{Flat Sandwich: } \frac{v}{\sqrt{2E}} = \left[\frac{M}{C} + \frac{1}{3}\right]^{-\frac{1}{2}} \qquad 2.3$$

$$\textit{Cylindrical Case: } \frac{v}{\sqrt{2E}} = \left[\frac{M}{C} + \frac{1}{2}\right]^{-\frac{1}{2}} \qquad 2.4$$

In some explosive and metal systems there may exist an air gap between the explosive and the metal casing, reducing the velocity to which the metal is accelerated. Computational work has suggested that the decreased velocity could be predicted by considering the explosive to have a reduced density [7]. This density would be equal to the mass of the explosive divided by the combined volume of the air gap and the explosive.

Combined loads

Generally, when an explosive device is functioned it produces both a blast wave and fragments. As such both the loading of the blast and the fragments must be considered. The velocity of the blast wave falls off more rapidly with distance than the velocity of the fragments. As such in the near field the blast will typically arrive before the fragments, whilst at a greater distance the fragments will arrive before the blast. At some middle distance both the fragments and the blast will arrive at the same time. The differences in time of arrival for the blast and fragments will change depending on the type of explosive used, design of the explosive device, and distance between the target and the explosive device.

As conventional weapons have the casing in contact with the explosive, the fragments produced have a very high velocity, resulting in them arriving at a similar time to the blast in the near field. For many targets this difference in time of arrivals is much shorter than the target's response time. It has been shown that a good initial estimation of the load imparted on a target in such a case can be made by superimposing the impulse of the fragment impacts with the impulse of the positive phase of the blast wave at the maximum blast pressure [8].

Ultra-High Performance Concrete

Ultra-High Performance Concrete (UHPC) is typically defined as a concrete for which the mix of constituents has been optimised so as to result in a high compressive strength. Often the range quoted for compressive strength in order for a concrete to qualify as UHPC is 150MPa. Concretes with extremely high compressive strengths in the rage of 600 to 800 MPa have been reported [9] however these require strictly controlled mixing and curing regimes at elevated temperature and pressures. As such, for large scale implementation, these concretes are currently economically nonviable. In some literature a distinction is made between UHPC not containing steel fibres and Ultra High Performance Fibre Reinforced Concrete. Here we will assume UHPC includes fibre reinforcing.

UHPC Formulations

The exact constituents and their proportions for UHPC mixes vary significantly. However, the core components remain relatively consistent [10]:

- Fine aggregates, such as sands, with the exclusion of larger aggregates typically found in concretes.
- A combination binder consisting of a cement and a fine pozzolanic reactive powder.
- A low water to binder ratio in the region of 0.2.
- A high proportion of superplasticiser to increase workability due to the low water to binder ratio.
- High strength steel fibres.

Aggregates

In order to increase homogeneity in UHPC mixes only fine aggregates are utilised. The most common of which is a fine silica sand with a maximum particle size of 0.5 mm [11] [12]. Studies have been undertaken to produce UHPCs with finer silicates such as ultrafine silica sands with particles sizes of 150 to 300 μm [13], quartz with particle sizes of approximately 10 μm [11], and other silicates with particles sizes of approximately 27 μm [10].

Binders

UHPCs typically utilise a hybrid binder that consists of a cement and a fine pozzolanic powder, most commonly, silica fume. The cement consists mainly of calcium silicates which react with the added water to produce calcium silicate hydrate (CSH) crystals between particles. Whilst the setting process is quite short, it can take a lot longer for optimal mechanical properties to fully develop. The silica fume is a near pure silica in the form of very small particles. These silica fume particles are approximately one hundredth the size of the cement particles [14]. This small size allows the silica particles to efficiently fill the voids around the cement particles, and the high surface area aids in them reacting to form more CSH crystals. These crystals are formed via a pozzolanic reaction in

which silicic acid (formed by the hydration reaction between the silica and water) reacts with calcium hydroxide.

Superplasticiser

In order to obtain higher compressive strengths in UHPC the water to cement ratio is reduced. This results in a dramatic reduction in the workability of the concrete mixture, which makes it difficult to produce homogeneous mixing and casting. A superplasticiser is added to improve the workability of the concrete mixture. The most frequently used superplasticiser is polcarboxylate ether [10] [11] [12].

Steel Fibres

Short steel fibres are added to the concrete mix towards the end of the mixing process. Their proportion is usually defined by their volume fraction in relation the concrete mix. The most commonly used fibres are 10-13 mm in length with a diameter of 0.2 mm, added in a proportion of approximately 2% [10] [11] [12]. Studies have also been undertaken to investigate the effect of longer steel fibres, different fibre fractions, and alternate fibre geometries [10] [13] [15].

Concrete Response to Blast

Concrete under static loading

The most common way to characterise concrete is by its uniaxial stress-strain relationship. Concretes are weak in tension with normal strength concretes typically having an ultimate tensile strength of less than one tenth of their ultimate compressive strength. Additionally concretes are very brittle when loaded in tension as the softening phase is steep once the peak load has been reached. The behaviour of concretes post-peak is generally characterised by the fracture energy of the concrete.

Strain Rate Effects

The mechanical properties of concrete, including strength, deformation capacity, and fracture energy, are not the same under a dynamic loading as they are under a static loading. This change in the mechanical properties is dependent on the rate at which the material is loaded and is known as the strain rate effect. When a sufficiently rapid and high amplitude dynamic load is applied to concrete, fracture, fragmentation and pulverization can occur. The response of the concrete is a process consisting of an initial elastic response, plastic flow, micro and macro crack formation, fragmentation, rubblisation and flow of rubblised particles [16].

To account for the change in concrete strength under elevated loading rates a Dynamic Increase Factor (DIF) is used. The DIF is the strain rate dependent proportional increase of the dynamic material properties relative to the static properties, and is most commonly used for ultimate strength. At different strain rates the ultimate compressive strength can more than double [17] and the ultimate uniaxial tensile strength can rise by a factor of seven [18].

Concrete under Blast Loading

Due to the ubiquity of concretes as a material in structures the response of concrete to blast loadings has been a topic of interest to military organisations for a long period of time. As such there exists a wealth of experimental data and numerical simulation on this topic. Much of this information is captured in technical design manuals [19] [20]. Concrete structural elements when exposed to blast will exhibit both global and localised behaviours, each related to different modes of

failure. Generally global effects have been studied by conducting far field (longer range between charge and test item) experiments, whilst local effects have been studied with experiments conducted in the near field. Experiments have consistently found that the most relevant material parameter that impacts deflection and damage most directly is the compressive strength of the concrete. The presence of reinforcement and fibres in concrete has been found to limit the extent of damage and scabbing.

The response of concrete structures to blast loading has been numerically simulated at a range of fidelities. High fidelity modelling has been conducted in simulation tools such as LS-DYNA [21] using a combination of Eulerian and Lagrangian methods. The combination of these methods is required to accurately model both the blast propagation and structural material response. Whilst this has produced very accurate predictions the computational strain and user effort required to utilise these models has limited their applicability to relatively small interactions of individual structural elements. For time-limited or larger investigations, such as the response of an entire building, simplified methods are required. Software tools such as the Vulnerability Assessment & Protection Option (VAPO) [22] utilise fast running Single Degree of Freedom (SDoF) methods to model each individual structural element. These SDoF methods can be enhanced with consideration for many effects including plastic hardening, softening, and pulse shape. Whilst not providing results to the same fidelity as the more computationally expensive tools, their ability to rapidly assess problems and investigate a much larger scope sees these tools being widely used outside of academia.

The damage to concrete structural elements can be rapidly estimated for a range of different blast loadings using Pressure-Impulse (P-I) diagrams, an example of which is shown below. These diagrams are iso-damage curves that specify the level of damage to the structural element given the peak pressure and impulse of a blast wave [23]. To generate these curves many numerical predictions or experimental tests are required. Due to the difficulties in obtaining large datasets from field tests the experimental cases are usually only used as validation points. Both SDoF analysis and finite element simulations have been used to generate P-I diagrams [24].

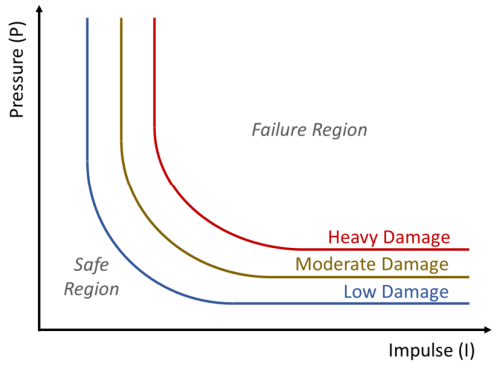

Figure 2: Diagram of a Pressure-Impulse diagram showing iso-damage curves

UHPC Blast Experimentation

Due to UHPC's relatively recent invention and the costs associated with modern blast testing, there is relatively little experimental work that has been conducted on UHPC response to blast.

Rebentrost and Wight [25] produced a report detailing a series of large-scale blast tests that were conducted on UHPC panels between 2004 and 2008. These tests utilised charges ranging in mass from 1 kg up to 500 kg. The UHPC panels suffered large deflections but produced little or no fragmentation. The added ductility of the UHPC resulted in panels developing a hinge capable of higher rotations than traditional reinforced concrete. It appears that no data was recorded during the events other than pressure histories. Panels were investigated post blast to measure total deflection and record qualitative observations.

Wu et al [26] undertook a study consisting of six panels consisting of two conventional reinforced concrete panels; two reinforced concrete panels retrofitted with a fibre reinforced polymer on the compressive face; one UHPC panel with no reinforcing; and one UHPC panel with steel reinforcement. Displacement was measured with a Linear Variable Displacement Transducer (LVDT) located at the centre of the rear surface of the panels. Pressure transducers were used to measure blast pressures at two locations per test but were omitted in higher load cases to avoid damage to the instruments. The variation in scaled distance between the tests makes comparison of UHPC performance against conventional concretes under blast loading difficult.

Barnett et al [27] have published work on a series of large-scale blast tests conducted on UHPC panels constructed by VSL Australia with a strength of 170-190 MPa. The panels were 3.5 m high and 1.4 m thick wide with a thickness of 100 mm. They were simply supported along the top and bottom and located in a 3.5 m by 3.5 m reflecting surface. 100kg TNT charges were detonated at distances of 7-12 m. Peak deflection was recorded at the centre of the panels. Deflections of 90-210 mm were recorded.

Li et al [28]undertook an experimental series in which four UHPC panels were tested against blast. Three different types of reinforcing were used, and the panels were tested at three different scaled distances. The large number of variables between tests, whilst understandable given the costs associated with testing, made it difficult to draw conclusions from the resulting data. The displacement of the panels was measured on the rear surface using Linear Velocity Displacement Transducers (LVDT). Reflected pressure was not recorded which complicated numerical simulation of the tests.

Yi et al [29] undertook a series of blast tests on 1m by 1m panels constructed from two different UHPC mixes with strengths of 200-220 MPa, one which did not contain steel fibres. Both panels contained nominal steel reinforcement. The panels were clamped on all four sides and tested against 15.88 kg ANFO charges at a distance of 1.5 m. Normal strength concrete panels were also tested but performed poorly. The UHPC panels survived the loadings with no visible cracks on the front surfaces. The rear surfaces did exhibit macro and micro cracking however significantly less cracking was observed on the panels containing steel fibres. This suggested that the steel fibres did play a role in improving the blast response of the UHPC panels. This test was the most instrumented UHPC blast test reviewed. LVDTs were used to measure the displacement of the panels over time, and strain gauges were used to measure the strain in both the concrete and the steel reinforcing rods. One improvement could have been multiple methods for measurement so as to gauge instrumentation accuracy.

Concrete Response to Fragmentation

In order to compare different materials the approximate penetrations depths are often given as factor of the depth of penetration for soft steel [30]. In the table below these factors are shown for some common materials.

Table 2: Relative penetration depths of common materials [30]

Material	Factor
Armour-plate	0.75
Soft Steel	1
Aluminium	2
Reinforced Concrete	6
Wood (Pine)	15
Sand	18
Water	50

Formula have been created to estimate the penetration of fragments into concrete, such as those produced by von Essen [31], Erkander and Pettersson [32], and ConWep [33]. Erkander and Pettersson's equation was produced from a curve fit to their experimental results and is shown below [32].

$$x = 2.88 \times 10^{-6} \times \sqrt[3]{m_f} \times \left(v_f - 170\right) \qquad 2.5$$

The equation produced by von Essen [31] is shown below. It calculates the penetration depth as a function of fragment mass and velocity, however it does not take into account variation in concrete properties.

$$x = 180 \times 10^{-6} \times v_f \sqrt[3]{m_f} \qquad 2.6$$

The equations used in ConWep are a function of the mass and velocity of the fragment, but also include the compressive strength of the concrete. The equations are shown below in imperial units.

$$x = \frac{0.95\, m_f^{0.37} v_f^{0.9}}{f_c^{0.25}} \; for\; x \leq 1.4 m_f^{\frac{1}{3}} \qquad 2.7$$

or

$$x = \frac{0.464\, m_f^{0.4} v_f^{1.8}}{f_c^{0.5}} \; for\; x > 1.4 m_f^{\frac{1}{3}} \qquad 2.8$$

A comparison performed by Erkander and Pettersson [32] of these equations to a wider series of experimental data suggests that ConWep estimates the penetration depth more accurately than the equations produced by von Essen. When constructing structures it may be necessary to design a wall that is sufficiently thick so as to prevent penetration by a fragment. A common assumption is that when a penetration depth of 70% of the thickness of a wall is predicted, once may expect perforation [34]. The thickness that is sufficient to prevent perforation, x_p, can be estimated by the following equation [34]:

$$x_p = x m_f^{0.033} + 0.91\, m_f^{0.33} \qquad 2.9$$

In this equation the x is the penetration calculated from the ConWep equations above, and m_f is the weight of the fragment in ounces.

Experiments conducted by Dancygier et al. [35] on UHPC samples with non-deforming projectiles were in reasonably close agreement with empirical predictions provided the compressive strength was well characterised. The presence of steel fragments in the UHPC was found to limit the extent of damage (width of craters) but did not have a significant impact on the depth of penetration.

Concrete Response to Combined Loadings

Due to the complexities of blast and fragmentation loadings they have historically often been considered separately. A review by Girhammar [36] found that when a structure was loaded by combined blast and fragmentation loads the damage generated by the loads was more significant than the sum of the damage generated by the application of the of loads independently. As such the blast and fragmentation loads should be considered synergistic. In a series of experiments Leppanen investigated the damage to concrete from a combined blast and fragmentation loading [37]. Concrete panels with dimensions 750x750x500 mm were tested against 1.3 kg octol and hexotol charges at ranges between 1.0 m and 0.6 m. Spherical pre-formed fragments with radii of 4 mm were accelerated by the explosives and impacted the panels with velocities varying from 1450 to 1650 m/s. Splitting tensile strength testing of drilled cylinders from the damaged panels found that concrete below the spalling zone did not have reduced strength. Leppanen suggested that it may be possible to separate the loads from the blast and fragmentation, allowing a structure to be analysed as a pre-damaged structure, and with the impulse from the fragment impacts combined with the impulse from the blast loading.

Forsen and Nordstrom [38] conducted a series of experiments investigating the response of concrete slabs to combined blast and fragment loadings. They found that deflection of the slabs under the combined loading could be well estimated by considering localised damage from fragment impacts and combining the impulses of the blast and fragmentation loadings. In this method the resistance of the concrete slab was reduced by considering the penetration depth of the fragments as reducing the effective thickness of the concrete slab. The impulse of the fragments was approximated by a triangular pressure wave.

Nystrom and Gylltoft undertook a numerical study to investigate the synergistic effects previously observed in numerous experiments [39]. They based the parameters for their study, both for the reinforced concrete structure, and for the blast and fragment loads applied, on Swedish Shelter Regulations [40]. They noted the need for experimental validation for their numerical simulations and a lack of suitable experiments with parameters similar to their own. Instead they utilised two separate experiments to calibrate their numerical model. One [41] to independently verify and calibrate the blast load and another for a single fragment impact into concrete [42]. SDoF analyses were conducted to determine the arrival times for the fragment and blast loads based on which loading times produced the greatest deflection. In these analyses the fragment loading was approximated by calculating the combined impulse of each fragment impacting the panel and representing this as a triangular pressure pulse with the same impulse. This pressure pulse had a width of 0.1 ms (approximately the penetration time for a fragment into the concrete) and a peak pressure of 22.5 MPa. It was found that the greatest deflection occurred when the loadings occurred simultaneously. The numerical analysis was then conducted in AUTODYN 2D and 3D [43] with a

Lagrangian solver technique, using the RHT concrete model and Johnson-Cook steel model. This analysis found that the local damage caused by fragment impacts occurred very early (within 0.25 ms) and was similar in both the combined loading and fragmentation only cases. This local damage resulted in a reduction to the effective thickness of the panel. It was observed that the mid-point deflection in the case of combined loading was larger than the sum of the deflections in the blast only loading and fragmentation only loading cases. This indicated a synergistic effect. Comparison to the SDoF analysis found that the results were similar for the blast only loading but the difference was larger for the fragmentation only and combined loading cases.

Grisaro and Dancygier produced a simplified approach for the analysis of combined blast and fragmentation loadings that considered the impulse of multiple fragment impacts and enabled evaluation of its significance relative to the blast load [44]. In their method the blast loading was determined by accounting for casing effects by determining an equivalent bare charge mass using the Hutchinson model [45], and then using the utilising the empirical equations for reflected blast impulse from the UFC design document [19] or with CONWEP [33]. The fragment loading was determined by estimating the impulse contribution of each individual fragment impact as a square pressure pulse, and then summing these pulses together over time. The fragment arrival times were determined with equations from the UFC design document [19]. The mass and velocities of the fragments impacting the panel were determined using Gurney equations and geometric considerations. The penetration time (used in determining the width of each individual fragment pulse) was determined using the UFC design document [19] and was dependant on the shape of the individual fragments. Grisaro and Dancygier compared results from their simplified methodology with experimental data and more complex numerical simulations and found their results “showed good agreement of the impacting fragment impulses [44]. This simplified approach assumes that: the panel is sufficiently thick such that fragment impacts do not produce rear surface effects; the fragments are non-deforming projectiles; and the impulse contribution of the fragment impacts can be approximated by the total momentum of the fragments impacting the panel area.

Research Gaps

From the preceding research it is apparent that significant effort has been invested in understanding concrete and its response to both blast and fragmentation, however the interaction of the material to these loadings is complex in nature. UHPC as a new material has only been utilised in a small number of experiments. These experiments have often consisted of only a few tests due to the cost associated with the testing. As such there has often been a high degree of variability between tests. Whilst some of these tests have shown that some of the empirical relationships previously established for conventional concretes can produce moderately accurate predictions at large scale distances [46] , at small scale distances their accuracy is significantly lower [47]This may be due to the inability of these relationships to capture the localised damage mechanisms of UHPC when loaded by contact and close proximity charges.

Whilst some work has been undertaken in understanding how combined blast and fragmentation loadings can synergistically load conventional concretes, the blast and fragmentation loadings that have been investigated have exclusively emulated the loadings produced by conventional munitions.

There have been no investigations in the open literature of the combined effects of blast and fragmentation produced by VBIEDs.

References

[1] A.-N. Z. C.-T. Committee, “Improvised Explosive Device (IED) Guidelines for Crowded Places,” Commonwealth of Australia, Camberra, Australa, 2017.

[2] W. Baker, 'Explosions in Air', University of Texas Press, Austin, USA, 1973.

[3] P. Bulson, 'Explosive Loading of Engineering Structures', CRC Press, Boca Raton, USA, 1997.

[4] R. Gurney, 'The Initial Velocities of Fragments from Bombs, Shell, and Grenades', Ballistic Research Laboratories, Aberdeen Proving Ground, Maryland, USA, 1943.

[5] J. Kennedy, 'Gurney Energy of Explosives: Estimation of the Velocity and Impulse Imparted to Driven Metal', Sandia Laboratories, Albuquerque, New Mexico, 1970.

[6] I. Henry, 'The Gurney Formula and Related Approximations for High-Explosive Deployment of Fragments', Hughes Aircraft Co. , Culver City, USA, 1967.

[7] T. Kennedy and J. Chou, 'Effects of gaps in explosive/metal systems', *14th International Pyrotechnics Seminar,* International Pyrotechnics Society, Boulder, USA*,* 1990.

[8] M. Nordstrom, 'Fragment Loading of Concrete Slabs', Technical Report, National Defense Research Establishment, Sudyberg, Sweden, 1992.

[9] P. Richard and M. Cheyrezy, 'Composition of Reactive Powder Concretes', *Cement and Concrete Research,* vol. 25, no. 7, pp. 151-1511, 1995.

[10] S. Kang, Y. Lee, Y. Park and J. Kim, 'Tensile fracture properties of an Ultra High Performance Reinforced Concrete (UHPFRC) with steel fiber', *Composite Structures,* vol. 92, no. 1, pp. 61-71, 2010.

[11] I. Yang, C. Joh and B. Kim, 'Structural Behavior of ultra high performance concrete beams subjected to bending', *Engineering Structures,* vol. 32, pp. 3478-3487, 2010.

[12] K. Habel and P. Gauvreau, 'Response of ultra-high performance fiber reinfocred concrete (UHPFRC) to impact and static loading', *Cement and Concrete Composites,* vol. 30, no. 10, pp. 938-946, 2008.

[13] S. Millard, T. Molyneaux, S. Barnett and X. Gao, 'Dynamic enhancement of blast-resistant ultra-high performance fibre reinforced concrete under flexural and shear loading', *International Journal of Impact Engineering,* vol. 37, no. 4, pp. 405-413, 2010.

[14] T. Holland, 'Structural behaviour of ultra high performance concrete beams subjected to bending', *Engineering Structures,* vol. 32, no. 11, pp. 3478-3487, 2010.

[15] K. Wille, A. Naaman and S. El-Tawil, 'Optimizing ultra-high-performance fiber-reinforced concrete', *Concrete International,* vol. 33, no. 9, pp. 35-41, 2011.

[16] S. Fichant, C. L. Borderie and G. Piljaudier-Cabot, 'Isotropic and anisotropic descriptions of damage in concrete structures', *Mechanics of Cohesive-frictional Materials,* vol. 4, no. 4, pp. 339-359, 1999.

[17] P. Bischoff and S. Perry, 'Compressive behaviour of concrete at high strain rates', *Materials and Structures,* vol. 24, no. 6, pp. 425-50, 1991.

[18] C. Ross, D. Jerome, J. Tedesco and M. Hughes, 'Moisture and Strain Rate Effects on Concrete Strength', *ACI Materials Journal,* vol. 93, no. 3, pp. 293-300, 1996.

[19] US Army Corps of Engineers, 'UFC 3-340: Structures to Resist the Effects of Accidental Explosions', USA Department of Defence, Washington, USA, 2008.

[20] Southwest Research Institute, 'A Manual for the Prediction of Blast and Fragment Loadings on Structures', USA Department of Defence, San Antonio, USA, 1980.

[21] *LS-DYNA Keyword User's Manual,* Livermore Software Technology Corporation, Livermore, USA, 2007.

[22] *Vulnerability Assessment and Protection Option (VAPO),* Defence Threat Reduction Agency, Raleigh, USA, 2013.

[23] T. Krauthammer, S. Astarlioglu, J. Blasko, T. Soh and P. Ng, 'Pressure–impulse diagrams for the behavior assessment of structural components', *International Journal of Impact Engineering,* vol. 35, no. 8, pp. 771-783, 2008.

[24] Y. Shi, H. Hao and Z. Li, 'Numerical derivation of pressure–impulse diagrams for prediction of RC column damage to blast loads', *International Journal of Impact Engineering,* vol. 35, no. 11, pp. 1213-1227, 2008.

[25] M. Rebentrost and G. Wight, 'Investigation of UHPFRC Slabs under Blast Loads', in *Designing and Building with UHPFRC*, John Wiley & Sons Inc., Hoboken, USA, pp. 363-376, 2013.

[26] C. Wu, D. Oehlers, M. Rebentrost, J. Leach and A. Whittaker, 'Blast testing of ultra-high performance fibre and FRP-retrofitted concrete slabs', *Engineering Structures,* vol. 31, no. 9, pp. 2060-2069, 2009.

[27] S. Barnett, S. Millard, G. Schleyer and A. Tyas, 'Blast tests of fibre-reinforced concrete panels,' in *Proceedings of the Institution of Civil Engineers*, London, England, 2010.

[28] J. Li, C. Wu and H. Hao, 'An experimental and numerical study of reinforced ultra-high performance concrete slabs under blast loads', *Materials & Design,* vol. 82, pp. 64-76, 2015.

[29] N. Yi, J. Kim, T. Han, Y. Cho and J. Lee, 'Blast-resistant characteristics of ultra-high strength concrete and reactive powder concrete', *Construction of Building Materials ,* vol. 28, no. 1, pp. 694-707, 2012.

[30] B. Engberg and S. Karevik, 'Fortikationshadbok del 1 (Verification Manual Part 1)', Defence Learning Centre, Stockholm, Sweden, 1987.

[31] W. v. Essen, 'Provisional instructions for reinforced concrete structures as protection against conventional weapons,' Swedish Fortification Agency, Eskilstuna, Sweden, 1973.

[32] A. Erkander and L. Pettersson, 'Concrete as a protective barrier against fragmentation impacts: Fragment impacts on plates made of different concretes,' Swedish Defence Research Agency, Stockolm, Sweden, 1985.

[33] ConWep, 'Conventional Weapons Effects from TM 5-855-1', United States Army Corps of Engineers, Omaha, USA, 2002.

[34] J. Leppanen, 'Concrete Subjects Subjected to Fragment Impacts', Chalmers University of Technology, Goteborg, Sweden, 2004.

[35] A. Dancygier, D. Yankelevsky and C. Jaegermann, 'Response of high performance concrete plates to impact of non-deforming projectiles', *International Journal of Impact Engineering,* vol. 34, no. 11, pp. 1768-1779, 2007.

[36] U. Girhammar, 'Brief review of combined blast and fragment loading effects', National Fortification Administration, Stockholm, Sweden, 1999.

[37] J. Leppanen, 'Dynamic Behaviour of Concrete Structures subjected to Blast, Fragment Impacts', Chalmers University of Technology, Goteborg, Sweden, 2002.

[38] R. Forsen and M. Nordstrom, 'Damage to Reinforced Concrete Slabs Due to the Combination of Blast and Fragment Loading', Swedish Defence Research Agency, Tumba, Sweden, 1992.

[39] U. Nystrom and K. Gylltoft, 'Numerical studies of the combined effects of blast and fragment loading', *International journal of Impact Engineering,* vol. 36, no. 8, pp. 995-1005, 2009.

[40] 'Shelter Regulations SR06', Swedish Rescue Services, Karlstad, Sweden, 2006.

[41] M. J and H. H, 'Numerical simulations of concrete beams - a principal study', National Defence Research Establishment (FOI), Tumba, Sweden, 2005.

[42] L. J, 'Fragment Impacts into Concrete - Experiments and Numerical Analyses', Chalmers University of Technology, Goteborg, Sweden, 2003.

[43] ANSYS, 'AUTODYN User Manual, Version 11.0', Century Dynamics Inc., Concord, USA, 2007.

[44] H. Grisaro and A. Dancygier, 'Characteristics of combined blast and fragments loading', *International Journal of Impact Engineering,* vol. 116, pp. 51-64, 2018.

[45] M. Hutchinson, 'The escape of blast from fragmenting munitions casings', *International Journal of Impact Engineering,* vol. 2, no. 36, pp. 185-192, 2009.

[46] G. Schleyer, S. Barnett, S. Millard and Wight, 'Modeling the response of UHPFRC panels to explosive loading', *Structures Under Shock and Impact,* vol. 113, no. 11, pp. 173-184, 2010.

[47] J. Li, C. Wu, H. Hao, Z. Wang and Y. Su, 'Experimental investigation of ultra-high performance concrete slabs under contact explosions', *International Journal of Impact Engineering,* vol. 93, pp. 62-75, 2016.

3. Research Objectives

The lack of work undertaken in quantifying VBIED effects is in part due to the costs associated with undertaking full scale VBIED tests. These costs are a result of both the need to utilise a vehicle, and a suitable testing range in which a device of this scale can be functioned. The loadings produced by VBIEDs, especially the fragmentation loadings, are highly variable and significantly different from those produced by conventional cased munitions. As such, when considering the impact of VBIEDs on structures the fragmentation loading is often ignored. It is unclear as to how significant this simplification is on the accuracy of the results produced.

This thesis, therefore, has two primary aims:

1. To accurately measure the pressure and fragmentation loadings of a VBIED surrogate charge, and the pressure loading of a comparative bare charge.
2. Investigate the deflection of structural panels, constructed from low and high technology materials, when subjected to the blast and fragmentation loadings produced by the VBIED surrogate and bare charges, and determine the significance of the VBIED fragmentation loadings.

Each of these aims formed the basis for a journal paper. These papers are included in this thesis as the following chapters:

- **Chapter 4: Quantification of blast and fragmentation loadings**
  - Published as: *Blast and Fragmentation Loading Indicative of a VBIED Surrogate for Structural Panel Response Analysis*
- **Chapter 5: Response of reinforced concrete panels to VBIED loadings**
  - Under Review as: *Response of conventional concrete and UHPC panels to blast and fragmentation loading indicative of a Vehicle Borne Improvised Explosive Device*

Statement of Authorship

Title of Paper	Blast and fragmentation loading of a VBIED surrogate for structural panel response analysis
Publication Status	☑ Published ☐ Accepted for Publication ☐ Submitted for Publication ☐ Unpublished and Unsubmitted work written in manuscript style
Publication Details	Mellen, P., Shanahan, C., & Bennett, T. (2019). Blast and fragmentation loading of a VBIED surrogate for structural panel response analysis. International Journal of Impact Engineering, 126, 172-184

Principal Author

Name of Principal Author (Candidate)	Phillip Mellen
Contribution to the Paper	Planned and undertook experimentation and data collection. Analysed and interpreted data. Wrote and edited manuscript and acted as corresponding author.
Overall percentage (%)	70%
Certification:	This paper reports on original research I conducted during the period of my Higher Degree by Research candidature and is not subject to any obligations or contractual agreements with a third party that would constrain its inclusion in this thesis. I am the primary author of this paper.
Signature	Date 23/01/19

Co-Author Contributions

By signing the Statement of Authorship, each author certifies that:

i. the candidate's stated contribution to the publication is accurate (as detailed above);

ii. permission is granted for the candidate in include the publication in the thesis; and

iii. the sum of all co-author contributions is equal to 100% less the candidate's stated contribution.

Name of Co-Author	Christine Shanahan
Contribution to the Paper	Supervised the development of the work and experimentation. Involved in manuscript evaluation and editing.
Signature	Date 23/01/19

Name of Co-Author	Terry Bennett
Contribution to the Paper	Assisted in structuring, evaluating, and editing the manuscript. Provided advice and input into data analysis.
Signature	Date 30/1/2019

4. Quantification of blast and fragmentation loadings

Published as: ***Blast and Fragmentation Loading Indicative of a VBIED Surrogate for Structural Panel Response Analysis.*** *Minor changes to appendices from published version (see Appendix C).*

P. Mellen[a,b,*], C. Shanahan[a], T. Bennett[b]

[a]Weapons and Combat Systems Division, Defence Science and Technology, Department of Defence, Australia
[b]School of Civil and Environmental Engineering, the University of Adelaide, SA, Australia

Abstract

This paper presents the results of an experimental investigation that was conducted at the Australian Department of Defence, Port Wakefield Proof and Experimental Establishment, in South Australia. The tests were undertaken to quantify the blast and fragmentation loads produced by both bare charges and a VBIED surrogate. The VBIED surrogate was designed to produce fragmentation indicative of a Vehicle Bourne Improvised Explosive Device and, in doing so, capture some of the properties of a device of this type that are significantly different to cased charges and conventional munitions. Incident pressures were recorded at 3, 4, and 5 m from the charge and reflected pressures were recorded at 3 m and across a 1.2 x 1.2 m flat panel to capture clearing effects of pressure history. The average velocity and distribution of fragment impacts were recorded for a panel of the same size.

Keywords: Vehicle borne improvised explosive device, blast, fragmentation.

Introduction

Vehicle Bourne Improvised Explosive Devices (VBIEDs) have been utilised as a weapon for hundreds of years with accounts of a gunpowder laden carriage used in an attempted assassination of Napoleon in 1800 [1], the well documented bombing of the Alfred P. Murrah Federal Building in Oklahoma City in 1995 [2] and the more recent bombing in Mogadishu that killed over 500 people [3]. In recent times the use of these types of devices by terrorist groups against civilian buildings and other structures has been a growing issue for many nations as the number of IED incidents globally increases [4,5].

VBIEDs consist of a large amount of explosive material within a vehicle, sometimes packed with inert materials (waste metal or ball bearings for example). When the explosive is detonated a high pressure blast wave is produced as well as numerous high velocity fragments. In the past, due to the complex nature of these loadings and limited documentation of their combined effects, the loadings have often been considered independently or together in an overly simplified manner [9].

VBIEDs are often used to damage high profile targets with a strong symbolic or logistical significance, or soft targets for which the primary aim is massive numbers of casualties [6]. A number of reports have highlighted the vulnerability of critical infrastructure to these types of attacks [7,8]. In order to

protect infrastructure, and reduce human casualties, a better understanding of how and why these devices cause such significant structural damage is warranted. A fundamental requirement of such an analysis is the elucidation of the blast and fragmentation loadings produced by these devices.

The effects of pure blast loadings on structures and structural materials has been well documented and much of this understanding has been captured in design documents [10,11] and simple software tools [12].

Understanding the generation of 'natural' fragments from VBIED detonations is intrinsically difficult due the variability in VBIED assembly and the complex construction of vehicles. Considerable work has been undertaken by many authors in understanding the generation of fragments [13-15], their size and speed distributions [14, 16-19], and how fragment generation affects the blast output [13, 20]. For steel cased explosives computational models have predicted the generation of fragment masses between 5 and 7 g [14, 15] and velocities ranging between approximately 1400 and 2000 m/s [14, 17-19]. The generation and acceleration of fragments has been shown to reduce the blast pressure output of a charge [13]. A number of variables effect how much the blast is reduced with the most dominant parameter being the ratio of the mass of the fragments to the mass of the explosive charge [20].

Whilst many of these models have been shown to be reasonably accurate they have only been developed for simple cylindrical, or spherical, metal casings entirely filled (no airgap) with explosive material. Devices of this type produce a detonation wave in the explosive material that is well coupled into the casing material, resulting in fragments of a small size and high velocity being generated. In VBIED construction there is often an airgap between the explosive material and portions of the body of the vehicle, resulting in larger, lower velocity fragments.

The effect of the projectile penetration into structural materials, in the absence of blast has been well documented [21-24]. The projectiles produce localised damage in the impact zone in the form of cratering, spalling, and cracking. This local damage can contribute to a reduction in the global load carrying capacity. This may be accounted for by considering the structure as having a decreased effective depth or width.

A review by Girhammar [25] has shown combined blast and fragmentation loads applied to a structure can cause responses that in some cases are more severe that the sum of the damage generated by the independent application of the loads. As such the blast and fragment loads should be considered synergistic. It has been suggested that the increased damage is due to the combination of spalling of the target material, and increased impulse, due to the fragment impacts [26]. A good estimation of deflection of a concrete slab has been obtained by accounting for the reduction in resistance of the slab due to the fragment impacts, and then adding the impulsive loading of the fragments to the positive impulse of the blast wave using a triangular wave [27]. The impulse contribution of the fragment impacts has been better described by substituting the triangular wave with a simplified model [28] that includes consideration for shape of the fragments. Due to the synergistic behaviour both types of loading must be considered concurrently when estimating VBIED loads.

Testing full scale VBIED's is difficult for two reasons; excessive cost and poor repeatability. Full scale tests require a new vehicle for each test and significant personnel time collecting and analysing fragments, the high cost of which typically results in very small test series. Additionally, the blast size and fragmentation hazard for this scale of test necessitates the use of a very large test range in order for the VBIED to fit within the hazard template. Poor repeatability in VBIED tests is due to the complex and non-uniform distribution of masses and materials within a vehicle, which results in a fragment distribution that varies greatly both spatially around the VBIED but also between tests utilising a similar VBIED. Due to this poor repeatability of VBIEDs the Defence Science and Technology Group (DST Group) designed a VBIED surrogate to produce a blast and fragment loading that would capture some of the key aspects of the loading produced by a VBIED, and allow an analysis of its differences to a conventional munition. Additionally, the surrogate was designed to be usable on a smaller test range and produce consistent fragment loading.

The aim of this work was to carefully characterise the loadings produced by both the DST Group VBIED surrogate, and a bare charge, to investigate the contribution of the VBIED fragments. By carefully characterising these loadings, the same loadings could be reproduced in a numerical simulation allowing for new materials to be tested in the "virtual laboratory" with only a smaller number of validation experiments required afterwards. This paper is the first step of that process and focusses on the experimental process and analysis of the loadings produced during trials in Port Wakefield, South Australia.

Materials and Methods

Experiments were carried out to; produce blast and fragment loadings indicative of a VBIED at a greater standoff, with consistency and repeatability, and to characterise these loadings with sufficient accuracy such that they could be reliably reproduced in modelling software.

VBIED Surrogate

The design of the VBIED surrogate was based on representative fragment masses and velocities obtained from a series of experimental tests undertaken by DST Group utilising a range of full scale VBIEDs. Frames from high speed video recorded during one of these tests are shown in figure 1. In figure 1 (a) the vehicle used for the VBIED is shown. In figure 1 (b) the shock produced by the detonation of the VBIED is visible. In figure 1 (c) and (d) the fragments produced by the VBIED are visible exiting the fireball. A wide distribution of fragment masses ranging from a few grams to tens of kilograms was recorded. The majority of fragments collected had masses of less than 200 grams. After investigation of the fragment data a fragment mass indicative of a typical fragment was identified and used in the design of the VBIED surrogate.

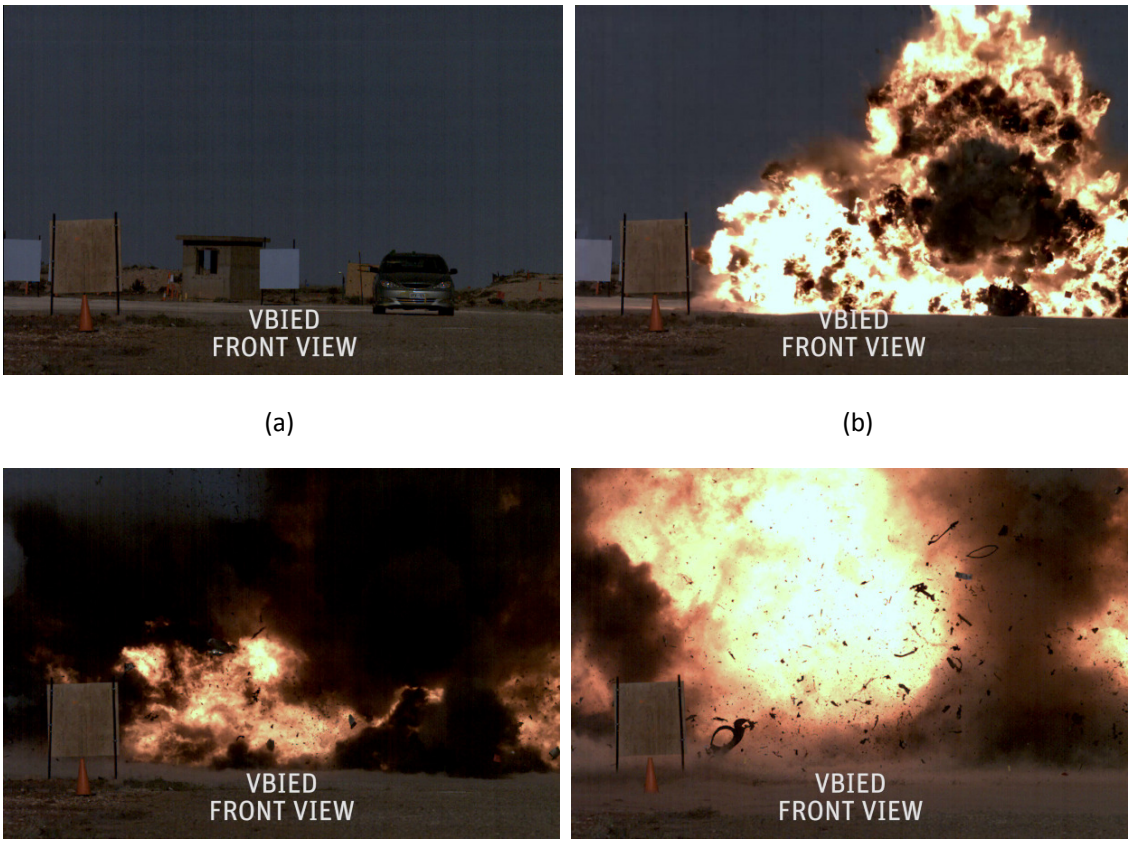

Figure 1: Frames from high speed video of a DST Group VBIED test showing blast and fragment production

Figure 2 depicts the schematic of the VBIED surrogate design used. It consisted of a 3 kg PE4 column surrounded by a ring of steel preformed fragments. The preformed fragments were 60 mm x 20 mm x 10 mm cuboids, with an average mass of 92g per fragment. The fragments were arranged in 10 rows with each row containing 22 fragments. This equated to 220 fragments per surrogate. The explosive charge mass was a compromise between optimising the fragment velocities and the blast pressure output.

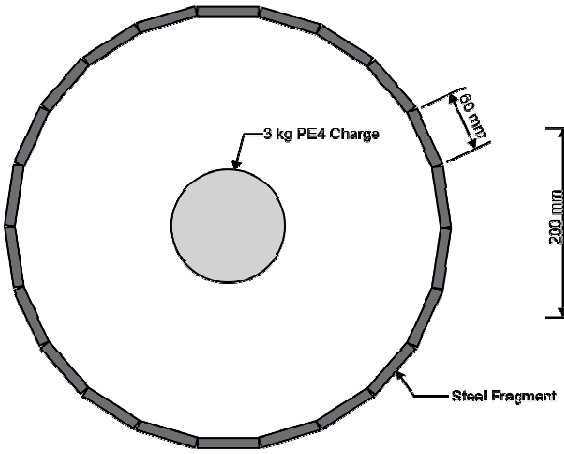

Figure 2 (a): Top view of the VBIED surrogate with steel fragments and PE4 charge

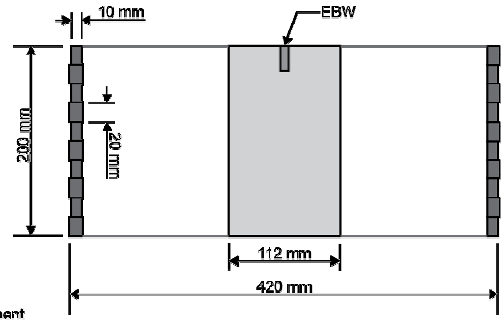

Figure 2 (b): Section view of the VBIED surrogate

An air-gap was included between the preformed fragments and the explosive charge to ensure poor coupling of the explosively driven shock wave to the fragments, similar to the construction of conventional VBIEDs. The size of the airgap was selected to reduce the velocity of the preformed fragments whilst maintaining the magnitude of the blast pressure.

Preliminary testing of the VBIED surrogate found the average fragment velocity to be approximately 400 m/s. Whilst this velocity was higher than the average velocity observed during the full scale VBIED tests it was well within the wide range of observed velocities. Whilst the VBIED surrogate did not accurately produce the broad range of fragment masses, velocities, and shapes generated by a full scale VBIED, it did capture some of the critical differences between a VBIED and a conventional munition whilst producing consistent loadings from test to test. These critical differences include larger fragment masses, slower fragment velocities, and a high fragment to explosive charge mass ratio.

Test Area

All experimentation was undertaken at the Department of Defence, Port Wakefield Proof and Experimental Establishment, in South Australia. Tests were conducted in an open air arena on a 12 x 12 m levelled concrete pad. The pad had “Unistrut” channels located at 0.4 m intervals along its length to allow for instrumentation stands to be accurately positioned and securely fastened. The explosive charges were located at the centre of the pad at a height of 2 m. The test rig was located such that the front face of a test panel would be at a distance of 3 m from the charge centre, with the midpoint of the test panel at a height of 2 m. All free field pressure gauges and fragment velocity instrumentation was also located with centres at a height of 2 m above the concrete pad. The layout of instruments on the concrete pad is shown in figure 3.

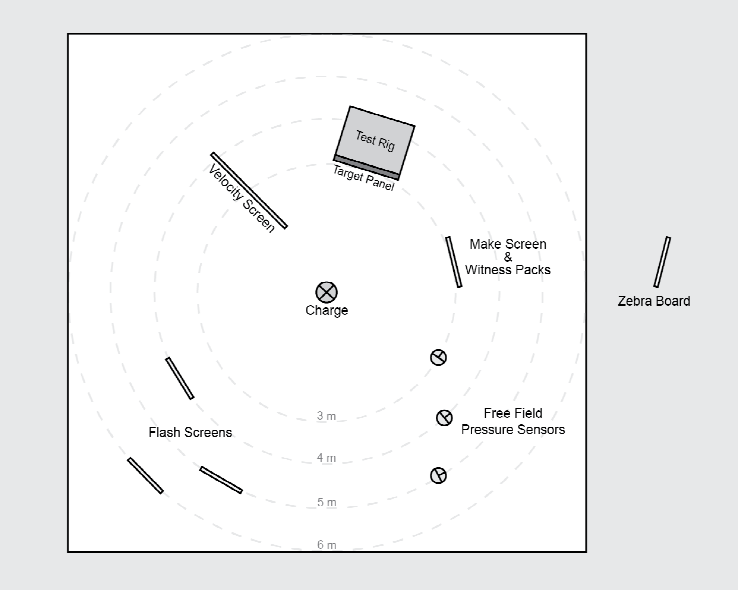

Figure 3: Overhead view of the test arena showing the layout of instrumentation relative to the explosive charge

Test Frame

The test frame, shown in figure 4, was constructed from welded mild steel tubular sections (shown in blue) and plates (shown in green) embedded in reinforced concrete (shown in grey). A mild steel bracket (shown in red) was used for mounting instrumentation inside of the test rig.

The test frame was designed to hold panels with nominal dimensions of 1.2 m x 1.2 m, and a variable thickness between 0.1 and 0.25 m. Previous work undertaken with DST Group determined that achieving a truly clamped boundary condition with no rotation at the constraint locations was not feasible. As such, test panels were held simply with near free rotation at the constraint locations, providing a well known boundary condition (simple-simple). This design choice was made to simplify future numerical modelling studies. The same constraint was utilised for the steel plate on which the reflected pressures were measured. The test frame was designed to occlude blast from the rear surface of the test panels to better simulate a structural component.

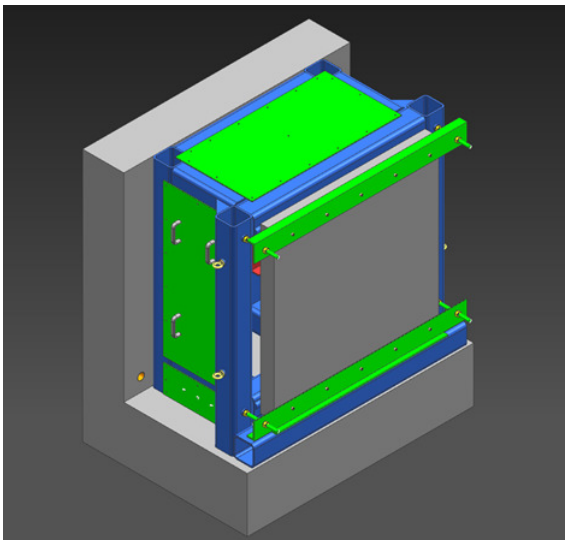

Figure 4 (a): 3D model of the test frame with the test panel in place

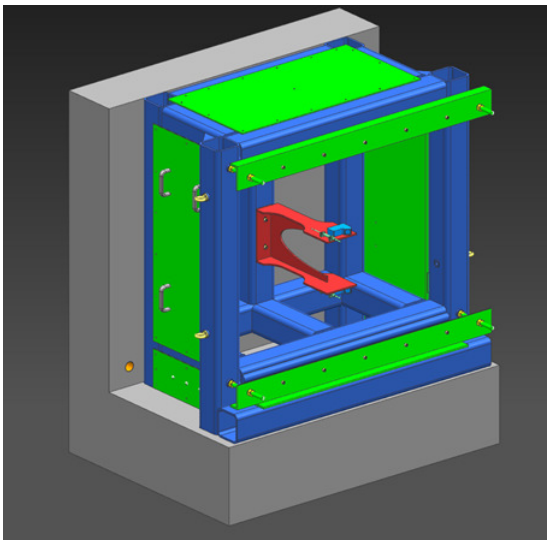

Figure 4 (b): 3D model of the test frame with the test panel removed

Pressure Gauges and Recording

The incident pressure, at various distances, and reflected pressure, at the test panel location, were recorded during the tests using Kulite XTL-190 gauges. The Kulite XTL-190 pressure transducer was a 4-wire Wheatstone bridge piezo-resistive transducer, with a very high natural frequency. Data was captured using Pacific Instruments 5871 transient data recorders. The 5871s were 14 bit analogue to digital recorders with integrated gain control, transducer signal conditioning, and wideband inputs. A sample rate of 1 million samples per second was selected to capture all aspects of the events. The pressure gauges were calibrated prior to the experiments by statically pressurising them from 5 % up to 100% of the peak range of the gauges in eight steps. The data recorders were triggered at time zero in conjunction with the electronic bridge wire (EBW) detonator firing circuit, and the high speed cameras.

To measure the incident pressure, three gauges were located at distances of approximately 3, 4, and 5 m from the charge centre at heights of 2 m above the concrete pad. They have been identified as P1, P2 and P3 respectively in the results. Exact measurements of standoffs for these gauges has been recorded in the appendix. The transducers were mounted in a shock absorbent Delrin plastic isolator and housed in 0.24 m aluminium knife edged discs (baffle plate) orientated at rights angles to the charge centre. The orientation and layout of these gauges during testing is shown in figure5.

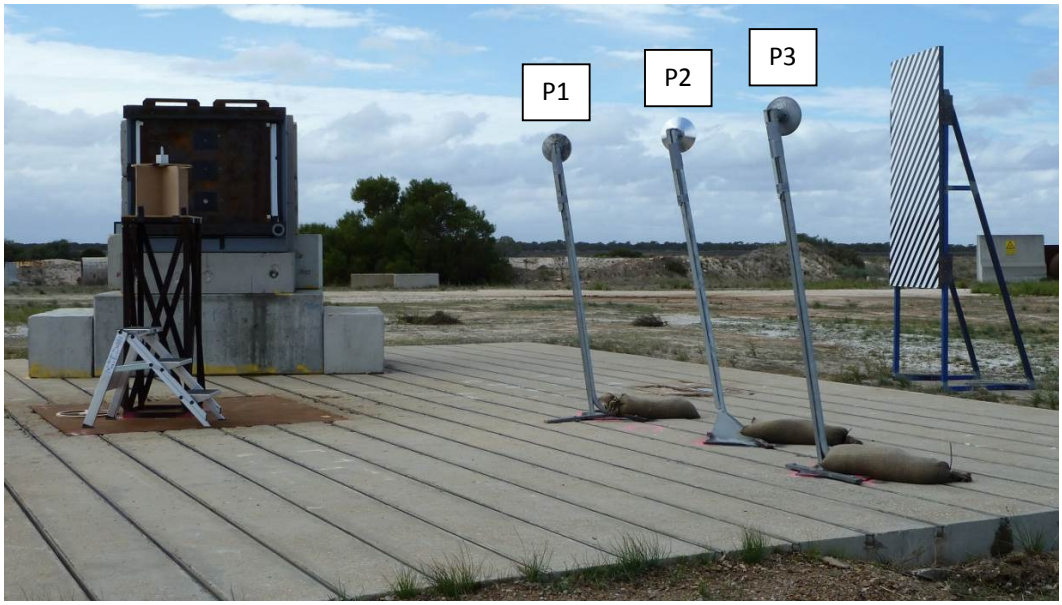

Figure 5: Locations of the incident pressure gauges prior to a test with gauge IDs shown

Reflected pressure for bare charge tests was recorded using a large steel plate secured in the test rig in the same manner as the test panels. This test plate had four gauges located at the plate centre, halfway between the centre and the top edge, halfway between the centre and the bottom edge, and halfway between the centre and the leftmost edge. This arrangement of gauges was designed to assess the clearing effects across the panel during the tests as well as the directionality and shape of the pressure waves. The location of these gauges and the respective IDs used in the results are shown in figure 6. The test plate was constructed from 30 mm thick mild steel with tubular steel reinforcing struts.

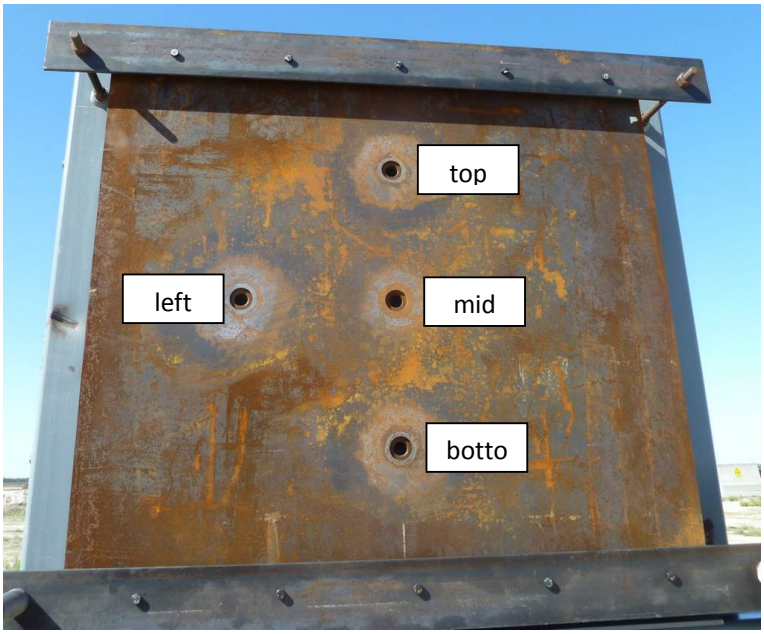

Figure 6: Test panel and reflected pressure gauge locations with gauge IDs shown

The steel test plate was not used during the VBIED surrogate tests due to the cost of replacing the plate after sustaining fragment damage. Instead a single pressure gauge was located at the centre of the make screen. The make screen had the same dimensions as the test panel and was located at the same distance from the charge centre.

Fragmentation Instrumentation

The velocity and distribution of the fragments were measured using a variety of methods which included a velocity screen, flash screens, make screens, and direct imaging.

A velocity screen was placed parallel to the predicted direction of the fragments. This screen was painted white with two fiducial markers 2 m apart, 2 m above ground (i.e. the same as the charge centre height). The fragments moving past the screen were imaged with a Photron SA5 Monochrome, running at 10,000 frames per second, with a resolution of 1024 x 512 pixels.

The flash screens consisted of three steel frames, each holding a 1.2 x 1.2 m aluminium sheet painted black. These frames were positioned perpendicular to the predicted fragment trajectories and imaged from behind with a Photron SAZ colour, running at 10,000 frames per second with a resolution of 1024 x 512 pixels. Initially these frames were placed at distances of 3, 4, and 5 m from the charge, however this was changed to 4, 5, and 6 m after it became apparent that the aluminium sheet was not capable of withstanding the blast pressure at 3 m. These panels gave a time of arrival for fragments at set distances, as well as a fragment distribution.

The make screens consisted of two conductive copper layers separated by a thin layer of insulating material. When struck by a steel fragment the two copper layers briefly connected electrically. This connection was recorded by the Data Acquisition system (DAQ). The make screen was located at a distance of 3 m from the charge centre. Initial tests found that unwanted signals were generated by the detonation products and RF noise in the blast area inducing a signal in the make screen. This interference was removed by the utilisation of an optical isolator to eliminate the DC connectivity of the make screen to the input of the DAQ.

Finally, the front of the test panel was imaged with a Photron SAZ colour running at various speeds. A zebra board was placed to one side of the panel and the camera was set perpendicular to predicted fragment trajectory. This camera allowed estimation of fragment velocity but also gave an insight into the interaction of the blast wave and subsequent secondary shocks on the test panel.

Four high speed cameras were used with a first surface mirror to ensure protection of the cameras from fragments. All cameras were triggered from a Delay Trigger Unit with a 90 V pulse from the Firing Point, and stepped down to a 5 V TTL pulse to the cameras.

Results

Testing was undertaken over the course of two experimental trials two months apart. Whilst the weather conditions were mildly different between these trials they had a negligible effect on the results as demonstrated by the low variation in the incident pressure traces.

Pressure matching for Charge Types

In order to better understand the contributions of the blast and fragmentation loads it was important that the bare charge reproduce, as accurately as was feasible, the pressure output of the VBIED surrogate. Based on simulations conducted in ConWep [12], it was predicted that a 1.8 kg bare charge would produce a similar pressure output to the VBIED surrogate at a distance of 3 m. In figure 7 the incident pressure history at a distance of 3 m is shown for the VBIED surrogate and the 1.8 kg bare charge. The pressure history of a 3 kg bare charge is also included for comparison to the VBIED surrogate as both contain 3 kg of PE4. The drop in peak pressure between the 3 kg bare charge and the VBIED surrogate demonstrated the extent to which the fragments in the VBIED surrogate reduced the blast pressure at the target panel. All pressure histories had their time zero set to the time of initiation of the Exploding Bridgewire Detonator (EBW).

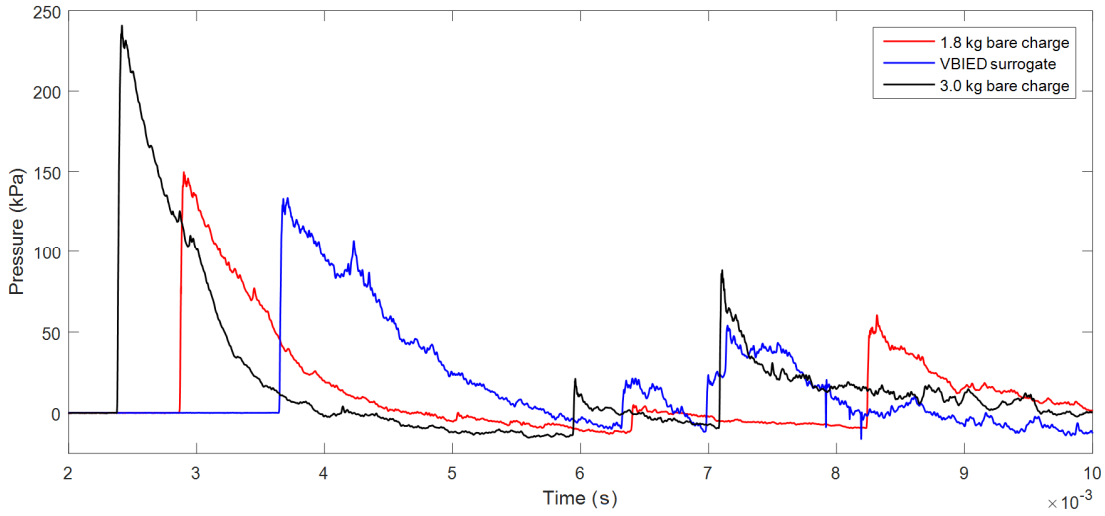

Figure 7: Incident pressure over time at a distance of 3 m for a 1.8 kg bare PE4 charge [red], and a 3 kg PE4 charge within the VBIED surrogate [blue], and a 3kg bare PE4 charge [black]

Considering only the first pressure peak (approximately 2.5 to 6 x10^{-3} s), it was observed that the peak pressure of the bare charge was slightly higher than that of the VBIED surrogate, however the impulse for the VBIED surrogate (108 Ns) was higher than that of the bare charge (87 Ns). The impulse was calculated by integrating the pressure history from the arrival of the initial shock to the start of the negative phase. It was decided that the pressure histories for the 1.8 kg bare charge and the VBIED surrogate were sufficiently similar for the requirements of these experiments. A closer match of both the impulse and pressure may have been achievable by utilising an explosive with a lower brisance however this was beyond the scope of this experimental series.

Incident Pressures

Incident Pressure traces were highly consistent for tests utilising the same explosive setup. In figure 8 the incident pressure at a distance of 3 m for a 1.8 kg bare PE4 charge is shown. Whilst there was some variation in initial timing, which may have been due to small triggering errors, the pressure history, particularly for the first pressure pulse was highly repeatable.

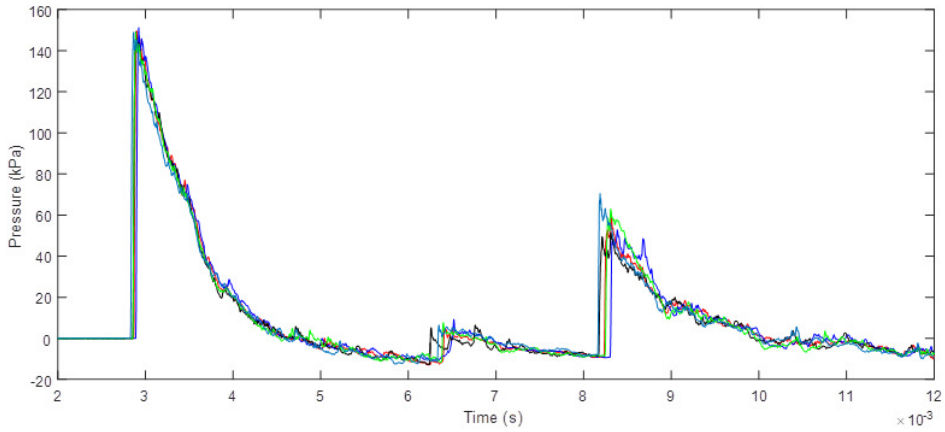

Figure 8: Incident pressure at a distance of 3 m from charge centre for 1.8 kg bare charges showing repeatability over five tests

In figure 9 the incident pressure at distances of 3 m, 4 m, and 5 m, is shown for a 1.8 kg bare PE4 charge (a), the 3.0 kg of PE4 charge within the VBIED surrogate (b), and a 3.0 kg bare PE4 charge (c).

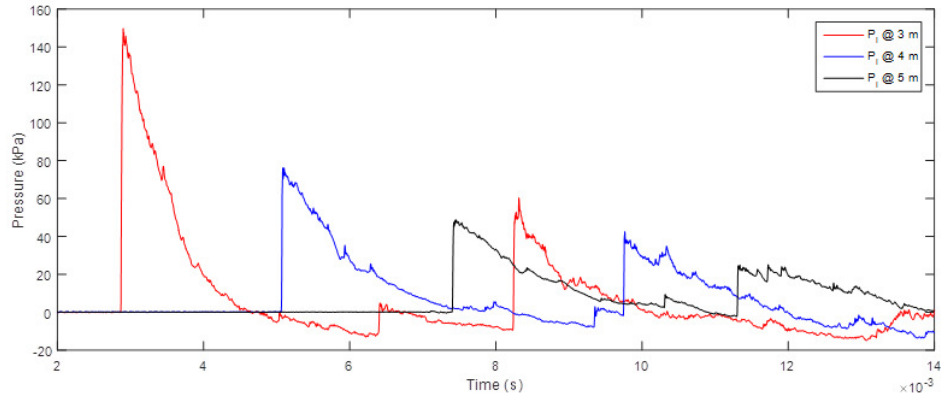

Figure 9 (a): Incident pressure at distances of 3, 4, and 5 m from charge centre for a 1.8 kg bare PE4 charge

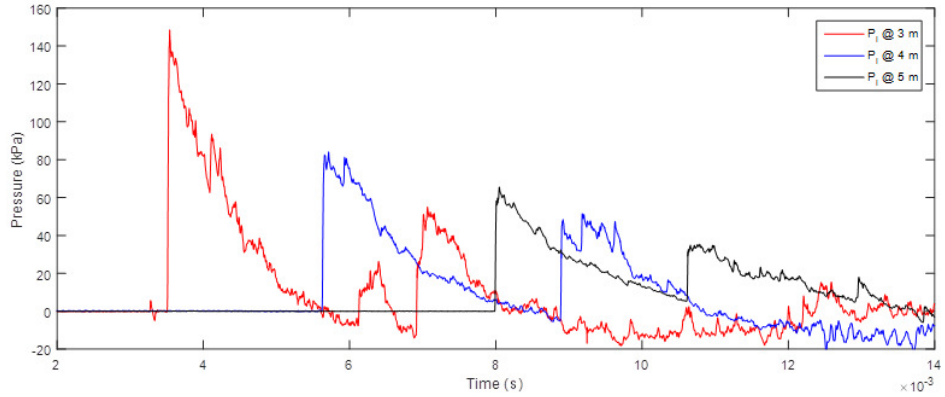

Figure 9 (b): Incident pressure at distances of 3, 4, and 5 m from charge centre for the VBIED surrogate

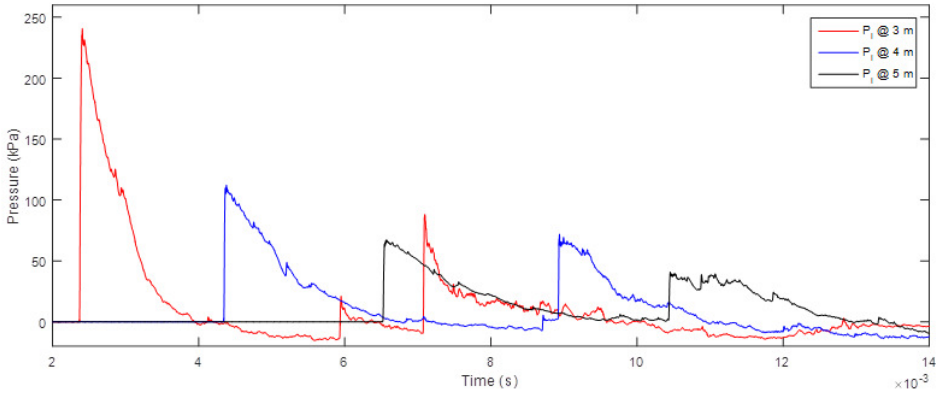

Figure 9 (c): Incident pressure at distances of 3, 4, and 5 m from charge centre for a 3kg bare PE4 charge

The incident pressures dropped as expected with distance. The difference in magnitude and time of arrival for the various charge types was readily apparent. Whilst the bare charges (*(a)* and *(c)*) produced relatively clean traces the VBIED surrogate traces contained much more noise. This noise is not surprising given that the blast wave had expanded around the preformed metal fragments, resulting in a less uniform wave.

A small shock was consistently observed at approximately 6 x 10^{-3} s, between the first shock and the ground reflected shock. This shock was weaker for the bare charges and more pronounced for shots utilising the surrogate. It was hypothesised that this wave was due to reflections off the charge stand. For the surrogate the ring of preformed fragments focused the blast onto the charge stand resulting in a greater amplitude for this reflected shock.

Reflected Pressures

Figure 10 shows the reflected pressure at four locations across the target plate for 1.8 kg and a 3.0 kg PE4 charges at a distance of 3 m. Pressure gauges were located at the centre of the panel [mid], halfway between the centre and the bottom edge of the panel [bottom], the leftmost edge of the panel [left], and the top edge of the panel [bottom], as shown in figure 6.

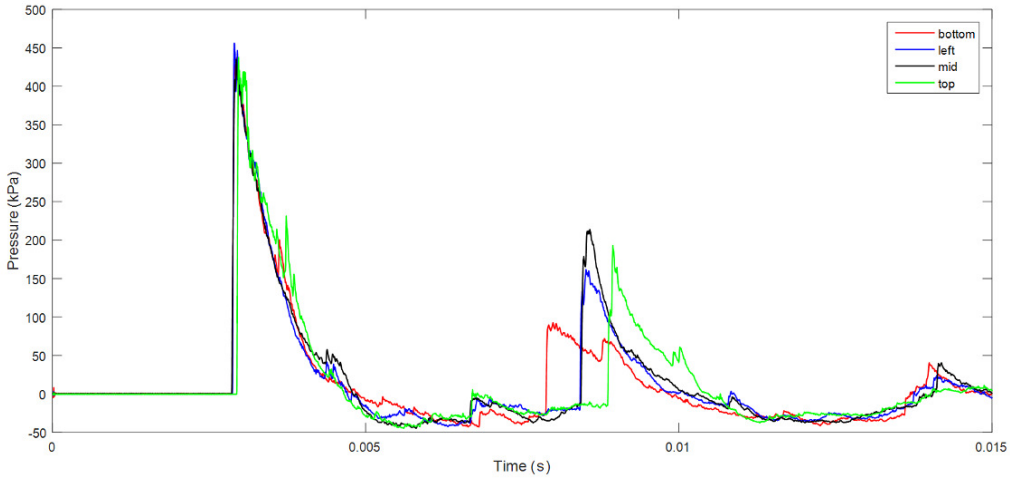

Figure 10 (a): Reflected pressures measured at various locations across a target plate at a distance of 3 m for a 1.8 kg PE4 charge

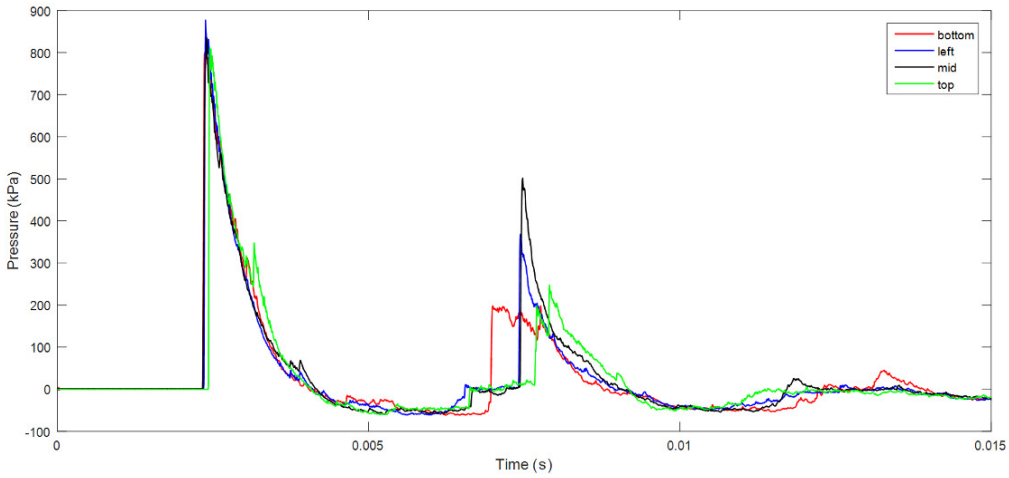

Figure 10 (b): Reflected pressures measured at various locations across a target plate at a distance of 3 m for the VBIED surrogate

The initial shock wave arrived at a similar time for all four pressure gauges, and similar pressure decays into the negative pressure period were observed. Whilst some differences in clearing were present in the pressure decay, these are relatively minor. Additionally, a slight spike was consistently observed in the pressure history of the top gauge as it decayed to approximately half its peak pressure. It was hypothesised that this small pressure spike was due to shock reflections off supports on the panel. The pressure histories diverged greatly for the ground reflected shock. The directionality of the ground reflected shock was apparent as it moved across the panel from the bottom towards the top edge. Across multiple tests the first pressure peak remained quite consistent with minimal variation, however the second pressure peak varied significantly between test shots. Whilst the times of arrival for this second shock were relatively similar the peak pressures fluctuated substantially. The time of arrival of the initial shock wave, and its peak pressure, for all pressure

gauges in each test of the experimental series are captured in the appendix. The horizontal standoff from the charge has also been included as this varied slightly during the experimental series.

Fragment Velocities

Fragment velocities were recorded using a number of methodologies including high speed video. In figure 11 frames from the camera used to film test panels are shown. The initial and ground reflected shock waves are visible prior to the impact of the fragments. In figure 12 frames from the camera used to film the velocity screen are shown.

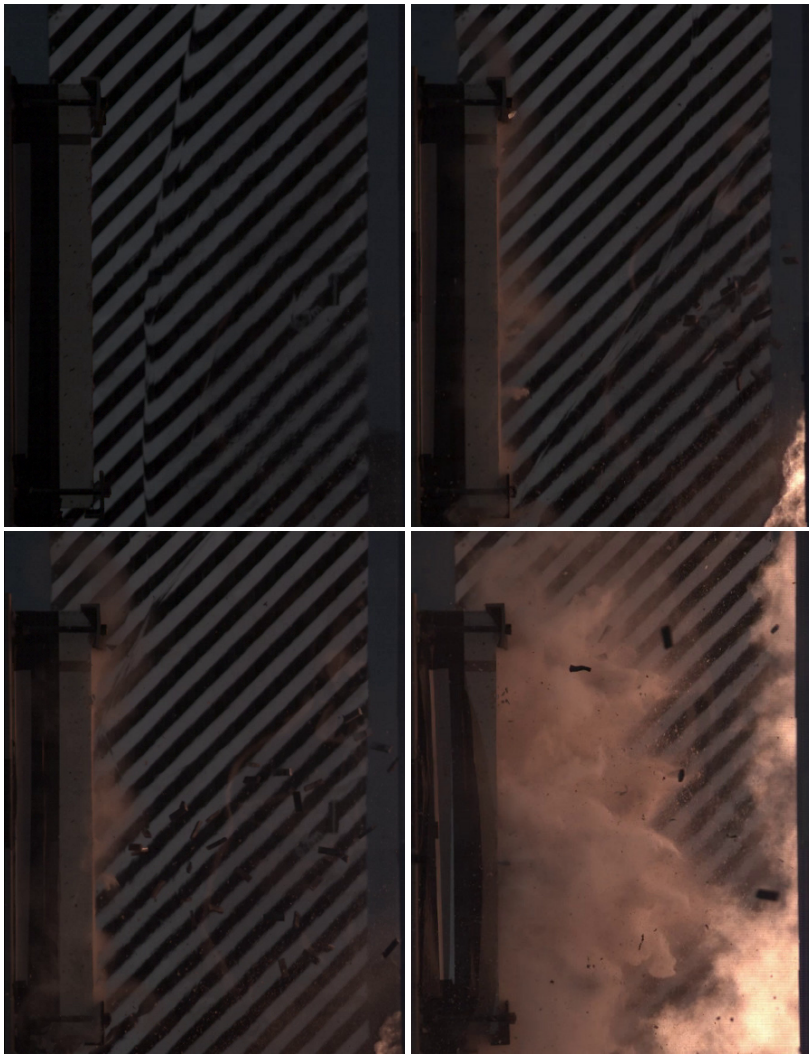

Figure 11: Frames from high speed video showing the shock wave and fragments striking a test panel

Figure 12: Frames from high speed video showing the fragments from the VBIED moving in front of, and damaging, the velocity screen

Table 1 shows a summary of the results of the fragment velocity measurements obtained by various experimental means. In early tests it was found that the supports of the make screen were insufficient to withstand the blast pressure, resulting in the screen moving during the test. This meant that the results were unreliable and only direct imaging and flash screen methods could be used for these tests. During later tests the make screen supports were strengthened and minimal deflection of the screen was observed. Good agreement was reached between the different methods. The velocity screen data was based on the first fragment cluster travelling parallel to the screen using a two-dimensional method. On the video image itself it was not possible to distinguish whether the fragments are traveling parallel to the screen or at an angle. However, it was assumed that the fragments moving fastest across the frame of the video were those travelling close to parallel with the screen. The velocity standard deviation for the velocity screen measurements was 10 m/s.

Table 1: Velocity measurements of fragments obtained by various measurement methods in m/s

Test ID	Velocity Screen		Make screen	Flash Screens			
	Fastest Fragment	*Second fastest Fragment*		*Ground Zero to Screen @ 3m*	*Ground Zero to Screen @ 4m*	*Ground Zero to Screen @ 5m*	*Ground Zero to Screen @ 6m*
04/3.1	363	363	-	-	355	341	-
05/3.1	388	375	-	408	379	377	-
07/3.2	385	376	383	-	370	362	361
08/3.2	362	348	364	-	367	373	363
09/3.2	368	362	379	-	380	379	370
10/3.2	373	365	381	-	361	355	341
11/3.2	362	360	384	-	380	363	351

Fragment Spatial Distributions

Whilst also being used to determine fragment velocities, the flash screens were used to record the number of fragments that impacted each screen, indicating density of fragment impacts. The flash screens were set up at distances of 4, 5, and 6 m from the charge centre. The screens had dimensions of 1.2 x 1.2 m, totalling an area of 1.44 m^2. Perforation of the flash screens during a test is shown in figure 13. The fragment density was determined using an average fragment mass of 0.092 kg. The number of fragment impacts and the resulting fragment density is shown in Table 2.

Figure 13: Still from high speed video showing fragment holes in flash screens lit from behind by the fireball of the VBIED surrogate

Table 2: Number of fragment impacts and density.

Test ID	Number of fragment impacts					Fragment density (kg/m^2)				
	Test Panel	*Make screen*	*Flashscreen at 4m*	*Flashscreen at 5m*	*Flashscreen at 6m*	*Test Panel*	*Make screen*	*Flashscreen at 4m*	*Flashscreen at 5m*	*Flashscreen at 6m*
07/3.2	12	11	7	5	3	0.74	0.70	0.45	0.32	0.19
04/3.1	9	-	12	5	2	0.56	-	0.77	0.32	0.13
05/3.1	10	-	10	6	4	0.62	-	0.64	0.38	0.26
08/3.2	9	9	7	4	5	0.56	0.57	0.45	0.32	0.32
09/3.2	8	10	7	5	3	0.49	0.64	0.45	0.32	0.19
10/3.2	11	11	8	3	4	0.68	0.51	0.51	0.19	0.32
11/3.2	11	9	7	3	4	0.68	0.58	0.45	0.19	0.32

The generally observed trend was a decline in fragment density at increasing standoff as expected. However, in some cases there were more impacts on the panel at 6 m than the panel at 5 m. This is due to the somewhat random distribution of the fragment impacts, and their low count at this distance.

Many fragments were recovered after the experiments. Fragments that impacted the soil around the test site exhibited no discernible deformation, only surface abrasion. The lack of deformation of these fragments indicates that the fragments were not deformed by the explosive blast. Fragments that had impacted concrete test panels and support structures exhibited minor deformation.

Conclusions

Whilst the pressure and impulse for the VBIED surrogate and bare charge setups could not both be simultaneously matched; a compromise was found that was sufficiently similar. Accurate histories were recorded for both incident pressures at various distances from the charge and reflected pressures across the target panel. These pressure histories were found to be highly consistent across a large number of tests. Clearing effects were observed in the reflected pressure histories, however they were relatively minor.

Fragment distributions and speeds were recorded. As such the impulse load generated by the VBIED surrogate from both blast and fragment loadings was able to be estimated for a panel areas of approximately 1.2 x 1.2 m. The fastest fragment speeds averaged approximately 370 m/s. As the fragments had a mass of 92 g this resulted in an energy of 12 kJ per fragment.

The data collected allowed for good quantification of both the blast and fragment loads produced by the VBIED surrogate and bare blast charges. The data for the pressure loadings was sufficiently consistent and accurate such that it can be used to reproduce these loadings in numerical simulations. The fragment loadings were accurately recorded and, whilst considerably more consistent than a VBIED, had substantial variation between tests. The data captured of these experiments could be used to reproduce an approximate fragmentation loading in a numerical simulation. Now that this first step has been successfully achieved, further experimental testing can be undertaken to investigate the effect these loadings have on conventional and new construction materials.

Appendix A: Summary of recorded pressures

Table A1: Summary of reflected pressures recorded throughout the experiment series.

Test ID	Charge Type	Gauge ID	Standoff from Charge (mm)	Time of Arrival (ms)	Positive Phase Duration (ms)	Peak Pressure (kPa)	Impulse per unit area *Positive phase only* (N.s/m^2)
07/3.2	VBIED Surrogate (3.0 kg)	Make Screen	2990	3.53	2.06	310	0.288
08/3.2		Make Screen	3000	3.54	2.15	405	0.287
09/3.2		Make Screen	3000	3.53	1.96	372	0.299
10/3.2		Make Screen	3020	3.57	1.96	381	0.282
11/3.2		Make Screen	3040	3.60	2.03	383	0.291
01/3.2	Bare Charge (1.8 kg)	Top	-	2.93	1.72	430	0.273
		Left	3000	2.87	1.83	454	0.269
		Mid	3000	2.86	1.93	432	0.283
		Bottom	-	2.87	2.01	434	0.276
15/3.2		Top	-	2.88	1.71	439	0.265
		Left	3010	2.81	1.83	464	0.261
		Mid	3010	2.80	1.91	451	0.278
		Bottom	-	2.81	1.91	455	0.276
01/3.1	Bare Charge (3.0 kg)	Mid	3025	2.38	1.87	908	0.474
02/3.2		Top	-	2.47	1.67	820	0.438
		Left	3000	2.37	1.74	809	0.434
		Mid	3000	2.42	1.86	824	0.452
		Bottom	-	2.43	1.75	852	0.465
14/3.2		Top	-	2.42	1.66	805	0.437
		Left	3010	2.35	1.75	866	0.437
		Mid	3010	2.33	1.84	827	0.450
		Bottom	-	2.33	1.71	823	0.460

Table A2: Summary of incident pressures recorded for VBIED surrogate tests.

Test ID	Charge Type	Gauge ID	Standoff from Charge (mm)	Time of Arrival (ms)	Peak Pressure (kPa)
04/3.1	VBIED Surrogate (3.0 kg)	P1	3049	3.81	131
		P2	4063	6.07	80
		P3	5060	8.28	54
05/3.1		P1	3017	3.66	135
		P2	4036	5.87	77
		P3	5033	8.29	59
07/3.2		P1	3010	3.71	133
		P2	4040	5.90	79
		P3	5010	8.21	60
08/3.2		P1	3010	3.65	134
		P2	4010	6.01	75
		P3	5010	8.18	57
09/3.2		P1	3020	3.54	145
		P2	4000	5.71	83
		P3	5010	8.05	65
10/3.2		P1	3020	3.63	131
		P2	4010	5.77	84
		P3	5020	8.19	60
11/3.2		P1	3020	3.58	115
		P2	4010	5.73	81
		P3	5020	8.10	74

Table A3: Summary of incident pressures recorded for bare charge (1.8 kg) tests.

Test ID	Charge Type	Gauge ID	Standoff from Charge (mm)	Time of Arrival (ms)	Peak Pressure (kPa)
01/3.2	Bare Charge (1.8 kg)	P1	3010	2.90	147
		P2	4030	5.10	75
		P3	5010	7.45	48
03/3.2		P1	3010	2.93	148
		P2	4030	5.11	74
		P3	5000	7.46	48
04/3.2		P1	3010	2.89	146
		P2	4030	5.09	77
		P3	5000	7.43	47
05/3.2		P1	3000	2.89	146
		P2	4030	5.10	75
		P3	5000	7.46	48
06/3.2		P1	3010	2.87	146
		P2	4030	5.08	75
		P3	5000	7.43	48
12/3.2		P1	3015	2.90	142
		P2	4005	5.02	77
		P3	5015	7.37	48
13/3.2		P1	3010	2.84	143
		P2	4000	4.90	78
		P3	5010	7.22	47
15/3.2		P1	3020	2.85	145
		P2	4000	4.87	81
		P3	5020	7.21	51

Table A4: Summary of incident pressures recorded for bare charge (3.0 kg) tests.

Test ID	Charge Type	Gauge ID	Standoff from Charge (mm)	Time of Arrival (ms)	Peak Pressure (kPa)
01/3.1	Bare Charge (3.0 kg)	P1	3029	2.43	225
		P2	4043	4.27	115
		P3	5041	6.33	60
02/3.1		P1	3022	2.40	221
		P2	4039	4.29	109
		P3	5038	6.52	67
03/3.1		P1	3028	2.37	223
		P2	4043	4.22	110
		P3	5040	6.35	68
02/3.2		P1	3010	2.41	238
		P2	4030	4.39	110
		P3	5010	6.59	66
14/3.2		P1	3010	2.39	240
		P2	4000	4.25	117
		P3	5010	6.42	70

Appendix B: VBIED surrogate limitations

It should be noted that the VBIED surrogate was not designed to reproduce every aspect of a real VBIED threat. Some of the aspects of VBIED loading that make it challenging to emulate; namely the high degree of variability in fragment velocity, material, and mass distribution; also make for a poor loading generator for experimental tests in which a consistent distribution is necessary between tests. Without moderate consistency it is not possible to compare the results of different tests. The VBIED surrogate discussed in this thesis was designed to use a single fragment that was indicative of approximately the most common fragment found in from data collected in previous VBIED field trials. The authors note that VBIEDs do consistently eject components of such a significantly different mass that these components should be considered independently. The most notable is the engine block which due to its large, dense, mass is often ejected predominantly intact. Typically, this will have a mass on the order of a thousand times greater than the most common fragment, and an ejection velocity many times slower. Due to the massively different properties of this individual component compared to the most common fragment its ability to load and damage structural elements should be considered independently.

Appendix C: Changes from published article

In response to feedback from reviewers of this thesis document this chapter was updated from the version published. The main body of the chapter is unchanged from the published version. Appendix A was updated to include additional information including the impulse and positive phase duration of the reflected pressures. Appendix B was added to provide comment on the limitations of the VBIED surrogate in representing all aspects of a VBIED threat.

References

[1] Lefebvre, G., 'Napoleon From Brumaire To Tilsit', Columbia University Press, New York, 1969.

[2] Oklahoma City Police Department, 'Alfred P. Murrah Building Bombing After Action Report', The Oklahoma Department of Civil Emergency Management, Oklahoma City, Oklahoma, 1995

[3] Reuters, 2017. 'Death toll from Somalia truck bomb in October now at 512. [ONLINE]' Available at: https://www.reuters.com/article/us-somalia-blast-toll/death-toll-from-somalia-truck-bomb-in-october-now-at-512-probe-committee-idUSKBN1DU2IC. [Accessed 10 December 2017]

[4] 'Developing an Empirical Understanding of Improvised Explosive Devices: A Social and Behavioral Science Perspective', National Consortium for the Study of Terrorism and responses to Terrorism, College Park, Maryland, 2009.

[5] Overton, I. et.al., 'Improvised Explosive Device (IED) Monitor 2017', Action On Armed Violence, London, 2017.

[6] Maniscalco P., 'Terrorism hits home', *Emergency Medical Service,* 1993; 22:31-2, 34-7, 40-1.

[7] ASCE, 'Protecting Infrastructure, in: Civil Engineering Research Foundation Monograph Series', American Society of Civil Engineers, New York, 2001.

[8] IEAust, 'Engineering a Safer Australia: Securing Critical Infrastructure and the Built Environment', Institution of Engineers, Canberra, Australia, 2003.

[9] Nystrom U. and Gylltoft K., 'Numerical studies of the combined effects of blast and fragment loading', *International Journal of Impact Engineering,* vol 36, 2009.

[10] United States of America, Department of Defense, 'Unified Facilities Criteria (UFC 3-340) Design and Analysis of Hardened Structures to Conventional Weapons Effects', US Army Corps of Engineers, Washington, DC, 202.

[11] American Society of Civil Engineers, 'FEMA 277 Improving Building Performance through Multi-Hazard Mitigation', Federal Emergency Management Agency, 1996

[12] 'ConWep', United States Army Corps of Engineers Protective Design Center, Omaha, Nebraska, 2002.

[13] Hutchinson M, 'The escape of blast from fragmenting munitions casings', *International Journal of Impact Engineering,* vol 36, 2009.

[14] Tanapornaweekit G. and Kulsirikasem W., 'Effects of material properties of warhead casing on natural fragmentation performance of high explosive warhead', *World Academy of Science, Engineering and Technology,* vol 5, 2011.

[15] Ugrcic M., 'Numerical simulation of the fragmentation process of high explosive projectiles', *Scientific Technical Review*, vol 63, pp 47-57, 2013.

[16] Moxes J. et. al., 'Experimental and numerical study of the fragmentation of expanding warhead casings by using different numerical codes and solution techniques', Defence Technology, vol 10, iss 2, pp. 161-176, 2014.

[17] Arnold W. and Rottenkolber E., 'Fragment mass distribution of metal cased explosive charges', *International Journal of Impact Engineering,* vol 35, 2008.

[18] Grisaro H. and Dancygier A., 'Numerical study of velocity distribution of fragments caused by explosion of a cylindrical cased charge', *International Journal of Impact Engineering,* vol 86, 2015.

[19] Huang G et. al., 'Axial distribution of Fragment Velocities from cylindrical casing under explosive loading', *International Journal of Impact Engineering,* vol 76, 2015.

[20] Grisaro H. and Dancygier A., 'On the problem of bare-to-cased charge equivalency', *International Journal of Impact Engineering,* vol 94, 2016.

[21] Leppanen, J., 'Concrete Structures Subjected to Fragment Impacts', Chalmers University of Technology, Sweden, 2002.

[22] Clegg R. et. al., 'The application of SPH techniques in AUTODYN-2D to kinetic energy penetrator impacts on multi-layerd soil and concrete targets', Eighth *International Symposium on Interaction of the Effects of Munitions with Structures,* Virginia, USA, 1997.

[23] Johnson G. and Beissel S., 'Computed radial stresses in a concrete target penetrated by a steel projectile', *Fifth International Conference on Structures Under Shock and Impact,* 1998.

[24] Leppanen J., 'Experiments and numerical analyses of blast and fragment impacts on concrete', *International Journal of Impact Engineering,* vol 31, 2005.

[25] Girhammar U., 'Brief review of combined blast and fragment loading effects', National Fortification Administration, Sweden, p. 264, 1999.

[26] Leppanen J., 'Dynamic Behaviour of Concrete Structures subjected to Blast, Fragment Impacts', Thesis, Chalmers University of Technology, 2002.

[27] Forsen R, Nordstrom M, 'Damage to Reinforced Concrete Slabs Due to the Combination of Blast and Fragment Loading', FOA report B 20101-2.6, Tumba, Sweden, Swedish Defence Research Agency, pp 12, 1992.

[29] Grisaro H and Dancygier A., 'Characteristics of combined blast and fragments loading', *International Journal of Impact Engineering,* vol 116, 2018.

Statement of Authorship

Title of Paper	Response of conventional concrete and UHPC panels to blast and fragmentation loading indicative of a Vehicle Borne Improvised Explosive Device
Publication Status	☐ Published ☐ Accepted for Publication ☑ Submitted for Publication ☐ Unpublished and Unsubmitted work written in manuscript style
Publication Details	Under review for the International Journal of Impact Engineering.

Principal Author

Name of Principal Author (Candidate)	Phillip Mellen
Contribution to the Paper	Planned and undertook experimentation, data collection and simulation. Analysed and interpreted data. Wrote and edited manuscript and acted as corresponding author.
Overall percentage (%)	70%
Certification:	This paper reports on original research I conducted during the period of my Higher Degree by Research candidature and is not subject to any obligations or contractual agreements with a third party that would constrain its inclusion in this thesis. I am the primary author of this paper.
Signature	Date: 23/01/19

Co-Author Contributions

By signing the Statement of Authorship, each author certifies that:

i. the candidate's stated contribution to the publication is accurate (as detailed above);

ii. permission is granted for the candidate in include the publication in the thesis; and

iii. the sum of all co-author contributions is equal to 100% less the candidate's stated contribution.

Name of Co-Author	Christine Shanahan
Contribution to the Paper	Supervised the development of the work and experimentation. Involved in manuscript evaluation and editing.
Signature	Date: 23/01/19

Name of Co-Author	Terry Bennett
Contribution to the Paper	Assisted in structuring, evaluating, and editing the manuscript. Provided advice and input into data analysis.
Signature	Date: 30/1/2019

5. Response of panels to VBIED loadings

Under review as: ***Response of conventional concrete and UHPC panels to blast and fragmentation loading indicative of a Vehicle Borne Improvised Explosive Device***

P. Mellen[a,b,*], C. Pienaar[a], T. Bennett[b]

[a]Weapons and Combat Systems Division, Defence Science and Technology, Department of Defence, Australia
[b]School of Civil and Environmental Engineering, the University of Adelaide, SA, Australia

Abstract

Vehicle Borne Improvised Explosive Devices pose a considerable security threat due to their ability to inflict mass casualties and damage structures to the point of collapse. As such, it is important to understand how the loads produced by these devices affect structural elements. This study investigated the response of reinforced concrete panels to bare blast, and combined blast and fragmentation loadings indicative of a VBIED. Panels were constructed from concretes with compressive strengths ranging from 22.5 to 160 MPa. Deflections were compared to simulations in SBEDS V5.1. A synergistic global response was observed and was dependent on the flexural stiffness of the panels and the timings between the blast and fragmentation loads.

Keywords: Vehicle Borne Improvised Explosive Device, Ultra-high performance concrete, blast, fragmentation.

Introduction

Vehicle Borne Improvised Explosive Devices (VBIEDs) continue to pose a major threat globally due to their ease of manufacture and ability to cause widespread damage [1]. These devices can cause casualties both directly and by damaging structures leading to collapse and further casualties [2,3]. In order to predict how these threats may damage buildings and to design for this, it is necessary to understand how these devices load structural elements. In this paper the structural elements of interest are panels constructed from a variety of conventional concretes and Ultra-High Performance Concrete (UHPC).

As with conventional munitions, VBIEDs produce both a blast loading from the detonation of the explosive material, and a fragment loading, from metal (and other material) components accelerated by the blast. In conventional munitions this fragment is consistent with small, high velocity fragments being produced [4]. VBIEDs produce a variable fragment loading due the inconsistency of their manufacture and improvised nature. The fragments produced vary greatly in mass, with the average being considerably larger than that of a convention munition [5]. Additionally, the average fragment velocity is consistently lower in VBIEDs, compared to conventional munitions, due to poor coupling between much of the fragmentation material and the explosive [5]. To understand how structures will respond, the effect of both the blast and fragment loadings must be well understood.

Pure blast loading has been extensively researched in the past with many experimental and numerical studies [6-9]. Idealised pressure histories, such as the Friedlander equation, and simple single degree of freedom analysis has been found to adequately predict global deflections and simple structural response [10]. Investigation of more intricate phenomena, including spallation and damage modes, has required the use of more complex tools including numerical hydrocodes [12,13].

Understanding the fragment loading requires an understanding of both the properties of the fragments (primarily mass and velocity) and their interaction with the structural material. Gurney developed a series of equations commonly used to predict the velocity of explosively driven metal fragments [13]. Design documents, such as UFC-3-340 [14], can be used to estimate the local damage generated by fragment impacts and their penetration depth. The momentum transfer from the fragment impact may also need to be considered. A numerical study by Crawford et al. [15] found that the impulse loading produced by fragment impacts was not negligible and must be considered in estimating structural response.

Analysis of explosive effects in which both blast and fragmentation loadings are considered together is rare due to the complexity of such an analysis. A relatively simple process for analysis of combined blast and fragment loading was described by Grisaro and Dancygier [16]. This process generates a pressure time history for the force applied by the impact of the fragments and results in a final loading that is a superposition of the pressure time history of the fragments and the blast. In this method the impulse of both loadings is captured. Nystrom and Gylltoft suggest that the combined loading of the blast and fragmentation can be synergistic, with the resulting damage being greater than the sum of the two loadings [17]. They state that the damage is due to three effects: the impulse loading of the blast, the impulse loading of the fragmentation, and the local damage (and hence reduced strength) from the fragment impacts [17].

To construct structures that are more resilient to these blast and fragmentation loadings, high strength materials are required. One option that has been found suitable for this application is UHPC. UHPCs are typically defined as concretes for which the mix of constituents has been optimised to produce a compressive strength in excess of 150 MPa. Strengths of up to 800 MPa have been reported however these require strictly controlled mixing and curing at elevated temperatures and pressures [18]. Whilst the mix constituents can vary, most mixes contain: a fine aggregate/sand to the exclusion of larger aggregates; a combination binder; a low water to binder ratio; and a high proportion of superplasticiser [19]. Tests of UHPC panels against blast have previously been conducted by Rebentrost and Wight [20], Wu et al. [21], Yi et al. [22], and Barnett et al. [23]. These tests found UHPC to have improved survivability against the blast loading when compared to conventional concretes.

Objective

The objective of this research was to experimentally study the response of conventional concrete and UHPC panels subjected to loadings from bare charges and VBIED surrogate charges. These surrogate charges were designed to reproduce key characteristics of VBIED loadings in a repeatable and low-cost fashion. The fragmentation and blast loadings produced by these surrogates, and their comparison to a bare charge, have been reported previously [24]. Concretes of strengths varying from 22.5 to 160 MPa were used to construct panels with thicknesses varying between 100 and 200 mm. This produced a range of flexural stiffnesses in the panels tested against both the bare and VBIED surrogate charges. One of the concretes tested was a UHPC as there is interest in its suitability in mitigating VBIED effects due to its previously recorded response to blast [20-23].

Materials and Methods

Test Panels

The dimensions and compressive strengths of the panels used in these experiments are summarised in table 1. All panels tested had a height of 1200 mm and a width of either 1200 or 1240 mm. The thickness of the panels varied between 100 and 200 mm. Three types of concrete with different compressive strengths were used for the panels. The first, referred to in this paper as ConConcrete, was intentionally designed to be a low strength concrete. This material was included to represent suboptimal building materials in resource constrained environments. The second, referred to in this paper as Tilt-Up concrete, was designed to be indicative of the material commonly used in tilt-up construction.

The third, referred to in this paper as UHPC, was a UHPC developed at the University of Adelaide. Phillip Visintin and his team developed this mix to utilise readily available Australian materials and low-cost manufacturing methods [25]. As such it has a strength lower than some UHPC mixes but does not require curing at controlled temperatures and pressures. High strength steel reinforcing fibres were included in the UHPC mix.

Table 1: Materials of test panels used in experimentation.

Concrete Type	*Thickness (mm)*	*Height and Width (mm)*	*Compressive Strength (MPa)*	*Quantity Tested*	*Reinforcing Mesh*
ConConcrete	150	1240 x 1200	22.5	2	Ø16 mm rod x 500 mm vertical spacing, Ø12 mm rod x 333 mm horizontal spacing at centre line
	200	1240 x 1200		2	
Tilt-Up Concrete	100	1200 x 1200	48	2	SL92 mesh at the centre line
	150	1240 x 1200		3	
Ultra-High Performance Concrete (UHPC)	100	1200 x 1200	160	6	Reinforcing Fibres and SL92 mesh at the centre line

All panels had reinforcing mesh located along the centreline of the panel. This placement was chosen to minimise the impact of the mesh on the panels response, whilst meeting safety requirements for transporting the panels. The SL92 mesh consists of 8.55 mm diameter rods with 200 mm spacings, in both the horizontal and vertical directions.

Test Frame

For these tests the concrete panels were held in a specially designed test frame. This frame was designed to hold concrete panels in such a way that; the edge conditions of the panels were consistent and well understood, and the blast was occluded from the rear surfaces of the panels. Due to the relatively small size of the panels, the blast would quickly diffract around the panel and equalize pressure on both sides of the panel if not occluded. Lightweight flashing and aluminium tape was used to ensure smaller gaps were sealed and did not allow blast or light into the interior of the test frame but did not restrict the motion of the panels during tests.

The final design for the test frame is shown in figure 1. The test frame was built from standard mild steel (shown in blue and green) of sufficient thickness to withstand multiple tests. Many of the

components exposed to blast and fragmentation were designed such that they could be replaced without requiring replacement of the entire test frame. The mild steel components were embedded into a reinforced concrete base and rear panel to minimise movement of the frame during blast loading. Additional concrete blocks were placed under the test frame to bring it up to the correct height, and behind the test frame to ensure movement was minimised.

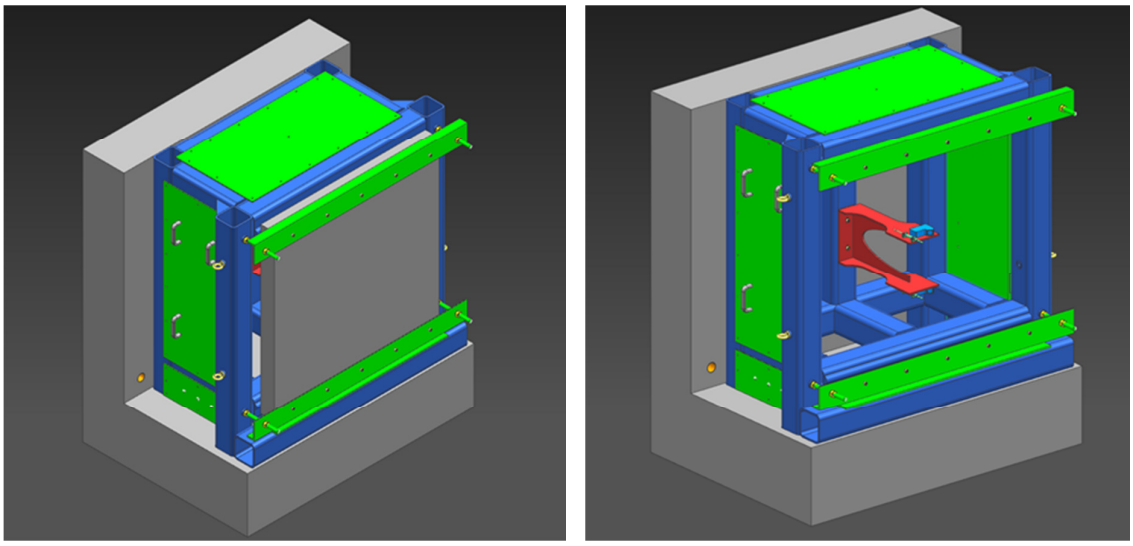

(a) (b)

Figure 1: Test frame with a concrete test panel in place (a) and without a test panel in place (b), showing concrete supports (grey), mild steel frame (blue), mounting brackets and blast exclusion panels (green), and instrumentation mounts (red).

The test frame was designed to hold the test panels such that the edge conditions were approximately simply supported at the top and bottom of the panels, and free along the other two edges. Previous tests conducted at DST Group found that fixed edge conditions were hard to produce due to the high stresses generated by blast loads. Test panels were held in the test frame by two clamps along the top and bottom of the panels. These clamps, and the test frame, had semicircular steel surfaces that contacted the concrete, holding it into the test frame, but minimising the restriction to bending in the panel. Figure 2 shows a concrete test panel in place in the test frame with the clamping bars visible at the top and bottom (a), and a closeup of the contact conditions between the test frame and the test panel (b).

(a) (b)

Figure 2: Test frame with concrete test panel in place and clamping bars affixed (a) and closeup of the contact conditions between the test panel and test frame (b).

Displacement Instrumentation

The displacement of each panel was recorded on the rear surface of the panel at both the half and quarter height with both Non-Contact Displacement Transducers (NCDT) and Linear Displacement Potentiometers (NDPs). Two types of instrumentation were used to improve confidence in the recorded displacement history. A typical displacement history for the NCDTs and NDPs at both the half and quarter heights is shown in figure 3. There is good agreement between the displacement recorded by the different instruments in the first 0.02 s after charge initiation. Later in the time histories the results from the different instruments begins to diverge due to dust generating noise in the NCDTs. This occurs well outside the time period of interest and did not impact the results of these tests. In future plots only the LDP data is shown due to the close correlation of the datasets during the time period of interest, and to improve clarity.

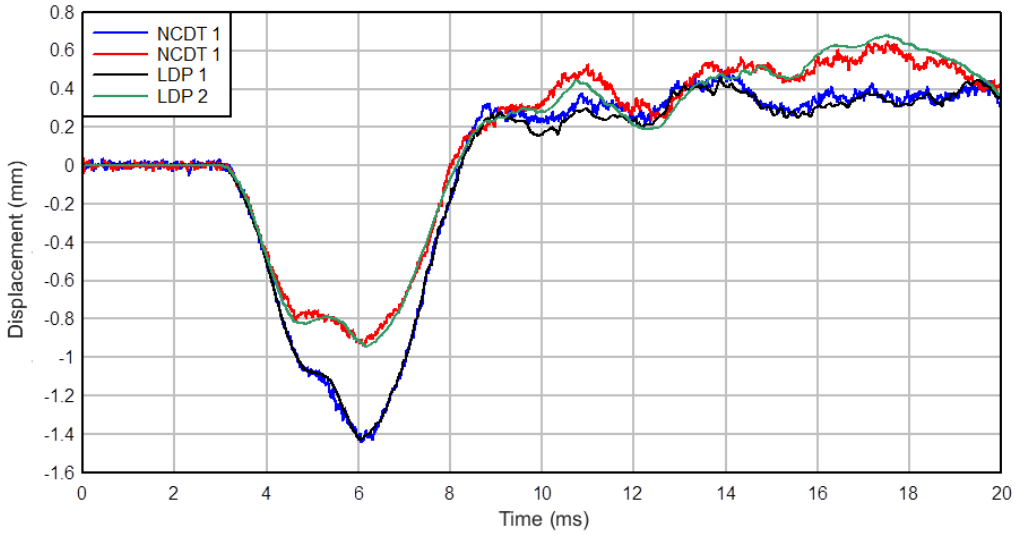

Figure 3: Displacement of UHPC panel when loaded by a 1.8 kg bare charge, as measured by a NCDT at the half height (blue), a NCDT at the quarter height (red), a LDP at the half height (black), and a LDP at the quarter height (green).

Blast and Fragmentation Loadings

The concrete panels in this series of experiments were loaded by two charge variations; a bare 1.8 kg PE4 charge, and a VBIED surrogate. All panels were tested with a charge standoff of 3.0 m. The loadings produced by these charges have been reported in greater detail previously [24]. The design of the VBIED surrogates was informed by a series of VBIED tests conducted previously by DST Group. These tests found VBIEDs produced a highly varied mix of fragments with a range of fragment velocities, masses and material compositions [5]. Despite this large variation in fragment properties some trends were determined and key differences between VBIED and conventional munitions were identified. The two main key differences were: VBIEDs typically produce a larger average fragment than conventional munitions; and VBIED fragments are typically slower, on average, than fragments produced by conventional munitions. The VBIED surrogates produce loadings that capture these key differences whilst maintaining consistency and reproducibility between experimental tests.

The VBIED surrogates consisted of a cylindrical 3 kg PE4 charge surrounded by a wall of preformed 0.09 kg mild steel preformed fragments. These fragments are significantly larger than those produced by a conventional munition. An airgap between the explosive and the fragments allowed for lower fragment velocities, to better match the velocities observed in previous VBIED tests. Using ConWep [26] the 1.8 kg bare PE4 charges were designed to match the pressure output of the VBIED surrogates. The aim of this was to expose the concrete panels to loadings with similar pressure components whilst varying the presence of fragments.

The reflected pressure was recorded for the bare charges by placing a steel plate with embedded pressure gauges into the test frame. Reflected pressure was not recorded at the test frame during the tests with concrete panels as the installation of gauges into the panels would have affected their response. Instead a gauge was placed in the centre of a screen, located at the same distance from the charge, with the same front surface dimensions. The reflected pressure was found to be reasonably consistent for each charge type. The incident pressure at 3, 4, and 5 m from the charge was recorded for all tests as another measure of loading consistency and was found to have very little variation [24].

In figure 4 the reflected pressure and impulse histories for the 1.8 kg bare charge (red) and VBIED surrogate (blue) are shown. In this figure, and all other time histories in this paper, the time zero corresponds to the initiation of the charge. The shown impulse was calculated from the recorded pressure history. Analysis of these histories showed that the 1.8 kg bare charge produced a higher peak pressure whilst the VBIED surrogate produced a greater impulse. Due to the stiffnesses of the panels tested it was predicted that the deflection would be predominantly dependent on the impulse, rather than the peak pressure, produced by the charges. The two pressure histories were deemed to be sufficiently similar for the requirements of this study. The dashed green line in figure 4 corresponds to the time at which the first fragment impacts the test panels. The exact time of each fragment impact varied from test to test, as did the fragment count. Analysis of recorded high speed video found that most fragment impacts occurred within 2 ms of the first fragment.

In the pressure history a second pressure peak is apparent for both the bare charge and the VBIED surrogate. Analysis of high-speed video found that this second peak was due to reflection of the primary shock wave reflecting off the ground of the test arena. During the planning stages for these experiments the effect of this reflection was considered. Unfortunately, the height of the charge could not be increased due to safety limitations in suspending the VBIED surrogate assembly and the test panels. The impulse history shows that the impulse contribution of this ground reflected shock is similar in magnitude to the contribution of the negative phase. The arrival time of this shock is similar to the fragments which complicates resolving their relative effects somewhat.

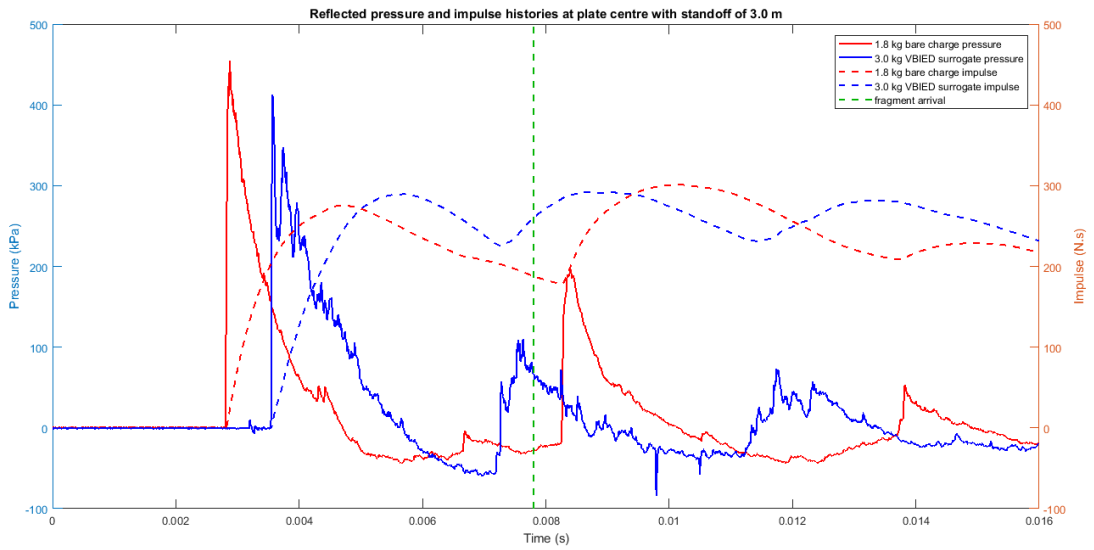

Figure 4: Pressure (solid line) and impulse (dashed line) histories for a 1.8 kg bare charge (blue) and a VBIED surrogate charge (red).

Results

Combined Impulse

The 1.8 kg bare charges consistently produced an initial pressure pulse with an impulse of 276 Ns. The VBIED surrogates produced an initial pressure pulse with an average impulse of 290 Ns. This impulse was expected to be more variable due to the fragments impeding propagation of the blast wave. The average fragment velocity at 3 m from the charge was found to be approximately 370 $m.s^{-1}$ with a standard deviation of 10 $m.s^{-1}$. The average fragment mass was 0.092 kg, giving an average momentum per fragment of 34 $kg.m.s^{-1}$. During the tests the number of fragment impacts on the panels varied between each test. The number of fragment impacts on each type of panel, and the approximate fragment impulse is shown in table 2.

Table 2: Number of fragment impacts and corresponding fragment impulse for various panels tested against VBIED surrogate charges.

Panel Material	*Thickness (mm)*	*Number of Fragment Impacts*	*Fragment Impulse (Ns)*
ConConcrete	150	12	283
	200	11	374
Tilt Up	100	9	306
	150	10	340
UHPC	100	8	272
		9	306
		11	408

ConConcrete Response

In figure 5 the deflection histories for the 150 mm (red) and 200 mm (blue) thick ConConcrete panels, when loaded by the 1.8 kg bare charge (solid line) and the VBIED surrogate (dashed line), are shown. It can be seen for both thicknesses that the initial deflection of the panels (prior to fragment arrival)

is greater for the VBIED surrogate. It is thought that this is due to the slightly higher impulse generated by the VBIED surrogate.

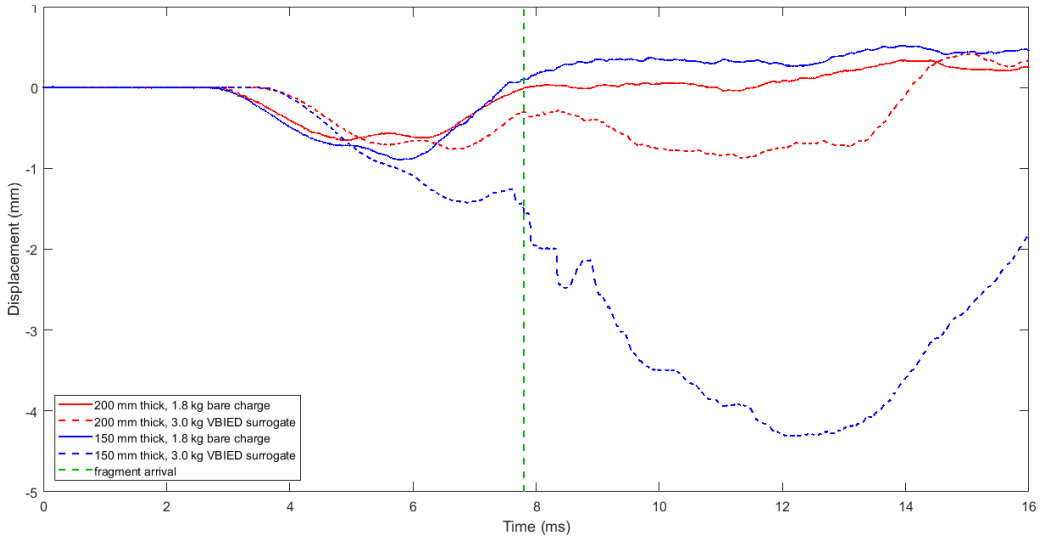

Figure 5: Displacement histories of 200 mm (red) and 150 mm (blue) thick ConConcrete panels when loaded by 1.8 kg bare charges (solid lines) or 3.0 kg VBIED surrogates (dashed lines) with approximate fragment arrival time (dashed green line).

For both loading types and panel thicknesses, the initial deflection, prior to the arrival of the fragments, had two separate peaks. It is unknown what caused this behaviour; however it was observed, with varying severity, in every test.

The contribution of the fragment loading to the panel deflection is readily apparent as the deflection changes rapidly at the time at which the fragments load the panels. It can be seen that for the 150 mm thick panel the fragment load occurs shortly after the panel has passed its peak deflection resulting in an increase of the peak deflection of approximately 180 %. For the 200 mm thick panel the increased flexural rigidity of the panel, due to its increased thickness, results in the fragment load occurring after the panel deflection has peaked and returned towards the undeflected state. In this case the peak panel deflection is only increased by approximately 20 %. However, this loading has generated a second deflection peak not observed in the deflection history for the bare charge.

Tilt-Up Concrete Response

In figure 6 the deflection histories for the 100 mm (red) and 150 mm (blue) thick Tilt-Up Concrete panels, when loaded by the 1.8 kg bare charge (solid line), and the VBIED surrogate (dashed line), are shown. It can be seen for both thicknesses that the initial deflection of the panels is slightly greater for the VBIED surrogate due to the higher impulse of the blast load.

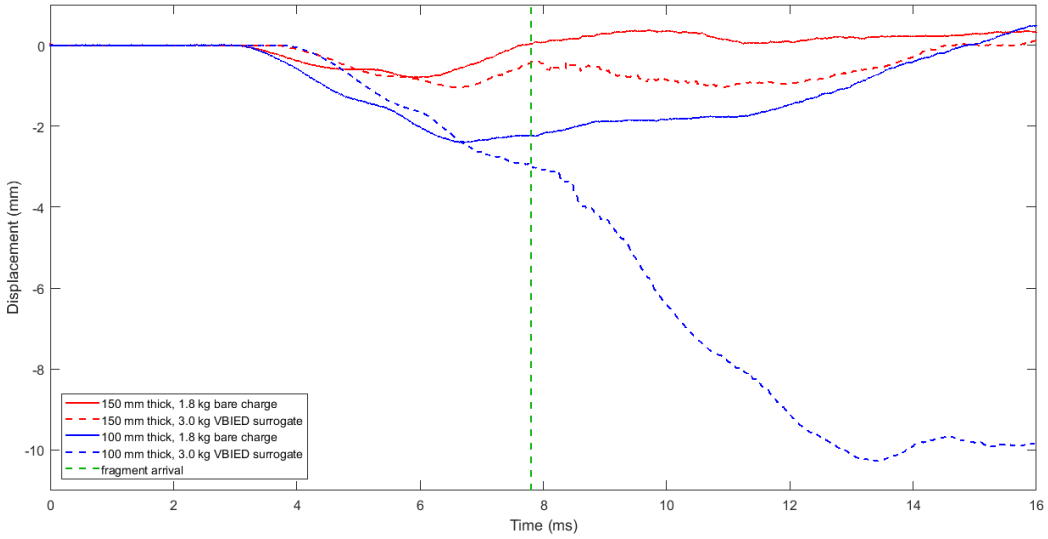

Figure 6: Displacement histories of 150 mm (red) and 100 mm (blue) thick Tilt-Up concrete panels when loaded by 1.8 kg bare charges (solid lines) or 3.0 kg VBIED surrogates (dashed lines) with approximate fragment arrival time (dashed green line).

Again, the contribution of the fragments is readily apparent. For the thinner 100 mm thick panel the fragment impact occurs as the panel is reaching its maximum deflection from the initial blast loading. Compared to the 1.8 kg bare charge, this results in the maximum deflection increasing by 330%. The 150 mm thick panel is stiffer resulting in a more rapid return in the deflection towards zero by the time the fragments impact the panel. Similar to the 200 mm thick ConConcrete panel, this results in no increase to the peak deflection but does produce a second deflection peak not observed for the 1.8 kg bare charge.

UHPC Response

In figure 7 the deflection histories for the 100 mm thick UHPC panels, when loaded by the 1.8 kg bare charge (red), and the VBIED surrogate (blue), are shown. For this panel material a single panel thickness was produced. However, six panels were constructed, allowing for two to be tested against the 1.8 kg bare charge and three to be tested against the VBIED surrogate. Again, the initial deflection of the panels is consistently greater for the VBIED surrogate. The response of the panels appears more consistent for the 1.8 kg bare charges with more variation in the deflection histories for the VBIED surrogates. This is not surprising given the disturbances caused by the shock waves diffracting around the fragments and the variability in the number of fragment impacts.

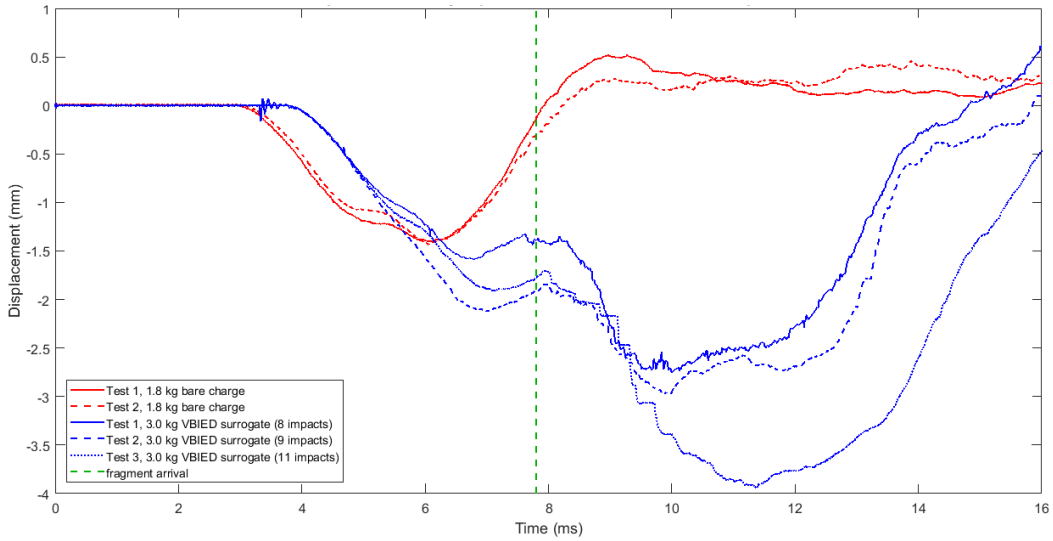

Figure 7: Displacement histories of 100 mm thick UHPC panels when loaded by 1.8 kg bare charges (red) or 3.0 kg VBIED surrogates (blue) with approximate fragment arrival time (dashed green line).

A large deflection due to the fragment impacts is observed. The fragments arrive shortly after the panel has reached its peak deflection due to the initial blast loading and has begun to return towards zero deflection. The loading of the fragments results in an increased maximum deflection. Additionally, the magnitude of this maximum deflection correlates to the number of fragments impacting the panel, with panels receiving the most fragment impacts having the largest peak deflection.

Deflection Comparison

The peak deflections for the various panels tested during experimentation is summarised in table 3 alongside the flexural stiffness for the panels. In figure 8 the maximum deflection of the panels is plotted against their flexural stiffness.

Table 3: Summary of peak deflections of all test panels.

Panel Material	*Thickness (mm)*	*Flexural Stiffness ($MPa.m^3$)*	*Peak Deflection Blast Only (mm)*	*Peak Deflection VBIED Surrogate (mm)*	*Increase in Peak Deflection*
ConConcrete	150	8.1	0.9	4.3	380 %
	200	19	0.6	0.9	50 %
Tilt-Up	100	3.5	2.4	10.3	330%
	150	12	0.8	1.0	25%
UHPC	100	6.5	1.4	3.9	180%

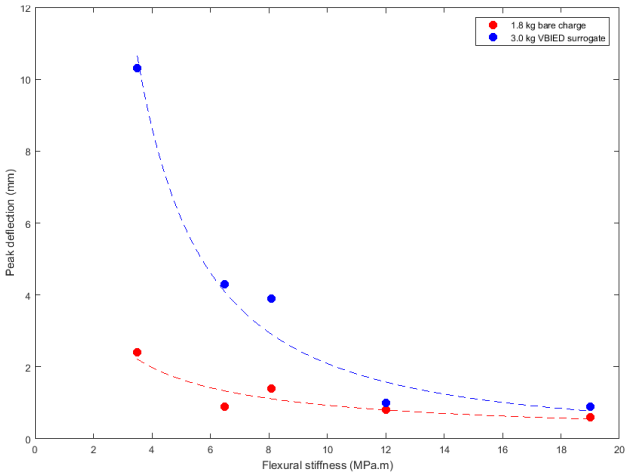

Figure 8: Maximum deflection of various concrete panels against flexural stiffness from experimental tests against a 1.8 kg bare charge (red) and a VBIED surrogate (blue)

For the panels with higher flexural stiffnesses the difference in peak deflection is negligible, however as the flexural stiffness of the panels drops the difference in peak deflection is dramatic. The natural frequency and response rate of the panels are dependent on the flexural stiffness. This supports the hypothesis that the thicker panels were sufficiently stiff that the panels had returned towards their nondisplaced location by the time the fragment loading is applied.

Numerical Simulation

Whilst combined blast and fragmentation loadings, and UHPC response to blast, have been modelled in the past it has usually been modelled using high fidelity finite element and computational fluid dynamics tools. Often in structural design these tools are not used due to their large computational times, the effort required in building a simulation, and their inability to model entire structures. Instead, fast running tools utilising Single Degree of Freedom (SDoF) models are often utilised. One such example is the Vulnerability Assessment and Protection Option (VAPO) which utilises SBEDS to model the effect of blast on individual structural elements [28]. Whilst SBEDS was not designed to model combined blast and fragmentation loading it was of interest to the authors to determine to what level of accuracy could it predict deflections for the combined loads.

SBEDS model

The dynamic response of the concrete panels was calculated using SBEDS V5.1 [27]. This program uses a single degree of freedom methodology, that is based on UF 3-340-01 [14], Army TM 5-1300 [28], and other sources, to estimate the response of structural elements to blast loading. The following material properties were used to model the response of the panels with the geometries described above.

Table 4: Material properties used in SBEDS calculations

Material	*Density (kg/m^3)*	*Poisson's ratio*	*Compressive Strength (MPa)*	*Elastic Modulus (GPa)*
ConConcrete	2400	0.167	22.5	24

Tilt-Up Concrete	2400	0.167	48	35
UHPC	2500	0.167	150	65
Steel Reinforcing	8000	0.33	275 (Yield Strength)	200

In order to model the combined blast and fragmentation an approach was adapted from similar approaches developed by Grisaro and Dancygier [16], and Nystrom and Gylltoft [17]. In these approaches the fragment impulse, I_{frag}, was assumed to be equal to the total momentum exerted on the panel by the fragments striking the panel, divided by the area of the panel, A_{panel}. This fragment impulse was assumed as acting evenly across the panel. It was then approximated by a pressure wave, here referred to as the fragment pressure wave, and added to the blast pressure history. Nystrom and Gylltoft utilised a simple triangular pressure wave [17] whilst Grisaro and Dancygier developed a model to predict the mass, velocity, and arrival time of each impacting fragment, assumed a square pressure wave for each individual fragment, and then summed these together to produce a complex pressure wave [16].

For the tests reported on here the mass, velocities, and impact locations were recorded for all fragments. This meant that experimental data could be utilised instead of an estimation model. The fragments were all weighed prior to construction of the VBIED surrogate and had a consistent mass of 0.09 kg per fragment. The average velocity of the fragments was measured to be 378 m/s. This resulted in an average impulse per fragment impact of 34 Ns. The number of fragment impacts per test varied between 8 and 12. Similarly to Grisaro and Dancygier each fragment impact was initially considered as a square wave, however, due to a limitation in the number of datapoints that could be utilised in SBEDS for custom pressure histories, all of the fragment impacts needed to be represented by a single pressure wave. A square pressure wave with a width of 1.4 ms and a variable height, based on the number of fragment impacts, was used.

Due to the limitation in datapoints available for representing custom pressure histories in SBEDS the recorded pressure histories needed to be simplified. For the bare charge this simplified pressure time history captured the peak pressure and impulse of the initial blast wave. For the VBIED surrogate tests the peak pressure and impulse of the initial blast wave was captured and the fragment impacts were represented by a square pressure wave described above. The simplified pressure histories are given in table 5 with table 6 giving the values required for the fragment impulse with variation in number of fragment impacts.

Table 5: Simplified pressure histories for SBEDS calculations

Bare 1.8 kg	*Time (ms)*	0.00	2.87	2.88	3.83	4.70	6.48	8.26	-
	Pressure (kPa)	0.00	0.00	455	62.0	0.00	-55.0	0.00	-
VBIED Surrogate	*Time (ms)*	0.00	3.54	3.55	4.96	7.80	7.81	9.20	9.21
	Pressure (kPa)	0.00	0.00	412	0.00	0.00	*x**	*x**	0.00

* x is the height of the square pulse in the pressure history that captures the impulse contribution of the fragments. It is dependent on the number of fragment impacts as described in table 6.

Table 6: Fragment impulse and corresponding fragment pulse height for SBEDS calculations

Number of Fragment Impacts	8	9	10	11	12
Total Fragment Impulse (Ns)	272	306	340	374	408
Height of Fragment Pulse x (kPa)	194	218	242	266	290

The results of the SBEDS simulation are shown alongside the experimental results for the ConConcrete panels in figure 9. For the 200 mm thick panel the deflection due to the blast is reasonably similar prior to the arrival of the fragments. After this point the SBEDS analysis overpredicts the deflection of the panels significantly.

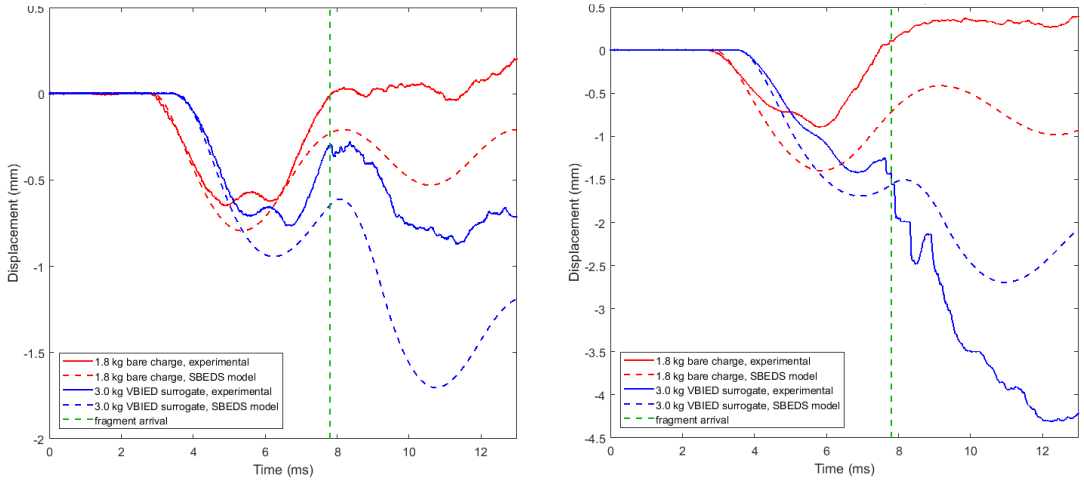

Figure 9: Comparison of experimentally recorded (solid lines) and numerically simulated (dashed lines) displacement histories of 200 mm (a) and 150 mm (b) thick ConConcrete panels when loaded by 1.8 kg bare charges (red) or 3.0 kg VBIED surrogates (blue), with approximate fragment arrival time (dashed green line).

For the 150 mm thick ConConcrete panel the SBEDS simulation again overpredicts the maximum deflection of the panel due to the pure blast. However, unlike the case for the 200 mm thick panel, the SBEDS underpredicts the deflection due to the impact of the fragments. There is a significantly larger deflection recorded in the experimental results than that predicted by the SBEDS simulation.

In figure 10 the comparison of the experimental results to the SBEDS simulations for the Tilt-Up concrete is shown. For the 150 mm thick panel the SBEDS simulation consistently overpredicts the deflection of the panels for both charge types. For the 100 mm thick panel the predictions from SBEDS are reasonably accurate in predicting the deflection prior to the arrival of the fragments. After the impact of the fragments the SBEDS simulation underpredicts the deflection of the panel. This is the opposite of the thicker panel but similar to the behaviour observed for the ConConcrete panels and the difference in prediction accuracy between the thick and thin panels.

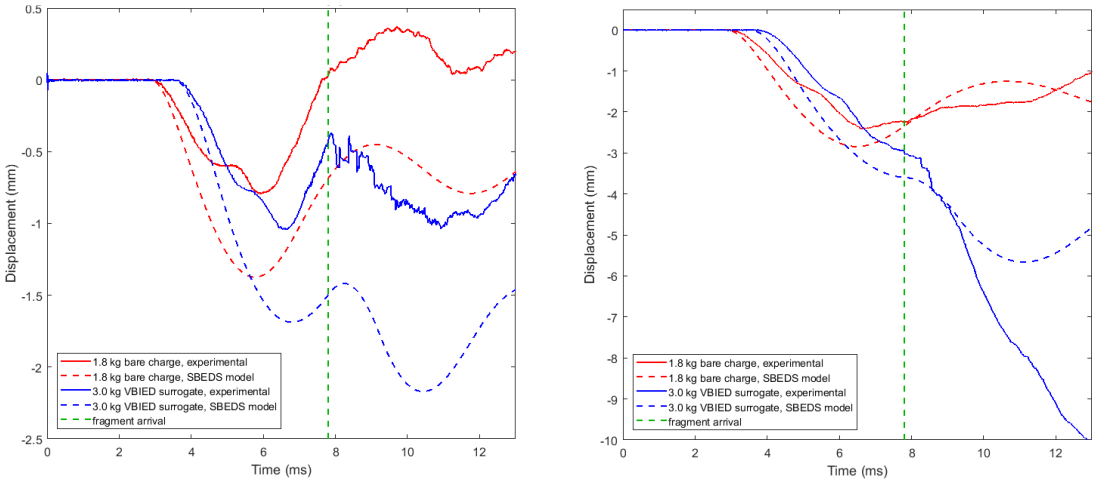

Figure 10: Comparison of experimentally recorded (solid lines) and numerically simulated (dashed lines) displacement histories of 150 mm (a) and 100 mm (b) thick Tilt-Up concrete panels when loaded by 1.8 kg bare charges (red) or 3.0 kg VBIED surrogates (blue), with approximate fragment arrival time (dashed green line).

In figure 11 the response of the UHPC panels is compared to the SBEDS simulations. For the bare charges the SBEDS prediction again overpredicts the deflection of the panels. For the VBIED surrogate tests SBEDS overpredicts the deflection of the panel initially when it is loaded by only the blast, but underpredicts the deflection when loaded by the fragments. This is consistent with the trend observed for the thinner panels.

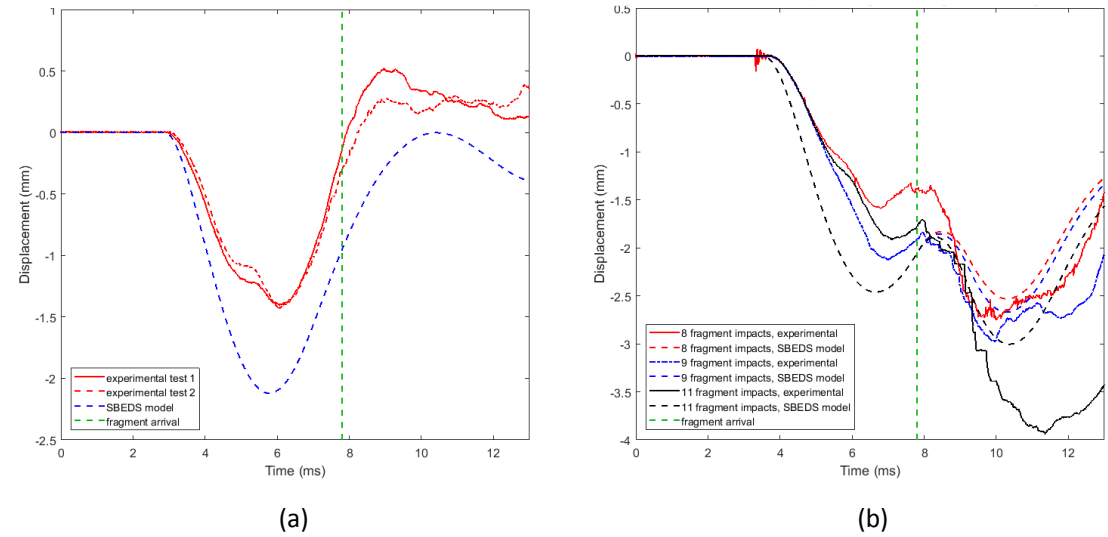

Figure 11: Comparison of experimentally recorded (solid lines) and numerically simulated (dashed lines) displacement histories of 200 mm (a) and 150 mm (b) thick ConConcrete panels when loaded by 1.8 kg bare charges (red) or 3.0 kg VBIED surrogates (blue), with approximate fragment arrival time (dashed green line).

For all the panels when loaded purely by blast the SBEDS prediction overestimated the deflection of the panels. This may partially be due to the edge conditions. Whilst the test rig was designed to hold the panels in place with minimal restriction to bending of the panels, the clamping will have provided some reaction moment. This could have slightly reduced the deflection of the panels in the experiments.

It was consistently observed that during fragment loading SBEDS overpredicted the deflection for the thicker panels and underpredicted the deflection for the thinner panels. It is thought that this may be due to the reduction in stiffness due to the damage caused by the fragment impacts. The maximum crater depth recorded during the experiments and crater depth predicted by UFC-3-340-02 [14] are shown in table 7. The crater depth was highly variable in the experiments and was heavily dependent on how close the impact was to the edges of the panel. UFC-3-340-02 predicted the crater depth reasonably well for the UHPC and Tilt-Up concrete, but overpredicted crater depth for the ConConcrete. If the crater depth was a sufficient percentage of the panels thickness it would have an impact on the stiffness of the panel. In SBEDS the impulse of the fragments was included but not the damage they caused to the panels. This could explain why the thinner panels, which had craters that compromised a greater thickness of the panel, deflected more in experiments than predicted by SBEDS.

Table 7: Fragment crater depths recorded during experiments and predicted using UFC-3-340-02

Panel Material	*Thickness (mm)*	*Maximum crater depth (mm)*	*Maximum crater depth (% of thickness)*	*UFC-3-340-02 Crater depth (mm)*	*UFC-3-340-02 Crater depth (% of thickness)*
ConConcrete	150	28	19 %	43	29 %
	200	29	15%	43	22 %
Tilt-Up	100	28	28 %	29	29 %
	150	18	12 %	29	19 %
UHPC	100	19 (avg)	19 %	16	16 %

Conclusions

Panels constructed from three concretes of varying strengths were tested against 1.8 kg bare charges and 3.0 kg VBIED surrogate charges. These charges had similar pressure outputs, but the VBIED surrogate produced fragments indicative of a VBIED. The displacement at the half and quarter heights of the panels was measured during the tests with multiple instruments recording consistent displacement histories. These displacement histories were compared to simulations in SBEDS. SBEDS consistently overpredicted the deflection of the panels when subject to blast loading, however it underpredicted the deflection for panels with lower flexural stiffnesses when subject to combined blast and fragment loadings.

The following conclusions can be drawn for the experimental results presented in this paper:

1. The impulse produced by the fragment impacts was sufficient to generate a global response for all panels tested. Therefore, it is vital that the contribution of fragments is considered when estimating the structural response of panels to VBIED threats.
2. The relationship between the flexural stiffness of the panel and the difference in time of arrival for the fragment and blast loads is highly significant on the maximum deflection of the panels:
    a. For panels with lower flexural stiffnesses the combined blast and fragmentation loadings produced sufficient damage to reduce the stiffnesses of the panels.
    b. Synergistic loading effects were only significant for panels with a sufficiently low flexural stiffness.
3. UHPC panels had lower deflections and shallower craters, than panels constructed of conventional concrete, when subjected to the loads produced by the bare charges and the VBIED surrogate charges. As such the material could be utilised to provide improved levels of protection against VBIED threats.
4. SDoF and similar simple numerical tools should be used with caution when attempting to estimate the response of panels to blast and fragmentation as localised damage will not be modelled and severe underprediction of deflection could occur.

References

[1] Overton I. et.al., 'Improvised Explosive Device (IED) Monitor 2017', Action On Armed Violence, London, UL, 2017.

[2] Luccioni B. et al., 'Analysis of building collapse under blast loads', *Engineering Structures*, vol 26, pp. 63-71, 2004.

[3] Osteraas J., 'Murrah Building Bombing Revisited: A qualitative assessment of blast damage and collapse patterns', *Journal of Performance of Constructed Facilities*, vol 20, 2006

[4] Curran D., 'Simple fragment size and shape distribution formulae for explosively fragmenting munitions', *International Journal of Impact Engineering*, vol 20, pp. 197-208, 1997

[5] Sunde J., 'Vehicle Borne Improvised Explosive Devices Effects Characterisation - 'Vehicle Roundup' Trial. Woomera', Technical Report, Defence Science and Technology Organisation, Edinburgh, Australia, 2011.

[6] Kingery C. and Bulmash G., 'Air blast parameters from TNT spherical air burst and hemispherical surface burst', Technical report, U.S. Army Ballistic Research Laboratory, Maryland, USA, 1984.

[7] Giannicola G., et al., 'Blast resistance assessment of concrete wall panels: experimental and numerical investigations', *International Journal of Protective Structures*, vol 5, pp. 348-366, 2014.

[8] Thiagarajan G. at al., 'Experimental and finite element analysis of doubly reinforced concrete slabs subjected to blast loads', *International Journal of Impact Engineering*, vol 75, pp.162-173, 2015.

[9] Shi Y. and Stewart M., 'Damage and risk assessment of reinforced concrete wall panels subjected to explosive blast loading', *International Journal of Impact Engineering*, vol 85, pp. 5-19, 2015.

[10] Morison C., 'Dynamic response of walls and slabs by single-degree-of-freedom analysis: a critical review and revision', *International Journal of Impact Engineering*, vol 32, pp. 1214-1247, 2006.

[11] Li J. and Hao H., 'Numerical study of concrete spall damage to blast loads', *International Journal of Impact Engineering*, vol 68, pp. 41-55, 2014.

[12] Wang W. et al., 'Experimental study and numerical simulation of the damage mode of a square reinforced concrete slab under close-in explosion', *Engineering Failure Analysis*, vol 27, pp.41-51, 2013.

[13] Gurney R., 'The initial velocities of fragments from bombs, shells and grenades', Technical report, U.S. Army Ballistic Research Laboratory, Maryland, USA, 1943.

[14] 'UFC-3-340-02 Structures to Resist the Effects of Accidental Explosions', With Change 2, Technical Report, US Army Corps of Engineers, Washington, USA, 2008.

[15] Crawford J. et al., 'Determining the effects of cased explosives on the response of RC columns', 21st International Symposium on Military Aspects of Blast and Shock (MABS 21), Jerusalem, Israel, 2010.

[16] Grisaro H. and Dancygier A., 'Characteristics of combined blast and fragments loading', *International Journal of Impact Engineering*, vol 116, pp. 51-64, 2018.

[17] Nystrom U. and Gylltoft K., 'Numerical studies of the combined effects of blast and fragment loading', *International Journal of Impact Engineering*, vol 36, pp. 995-1005, 2009.

[18] Richard P. and Cheyrezy M., 'Reactive powder concretes with high ductility and 200 – 800 MPa compressive strength', *Concrete technology: Past, present, and future, Proceedings of V. Mohan Malhotra Symposium,* vol 144, pp. 507-518, 1994.

[19] Wang C. et al., 'Preparation of ultra-high performance concrete with common technology and materials', *Cement and Concrete Composites*, vol 34, pp. 538-544, 2012.

[20] Rebentrost M. and Wight G., 'Investigation of UHPFRC Slabs under Blast Loads', Designing and Building with UHPFRC, John Wiley & Sons Inc., Hoboken, USA, 2013.

[21] Wu C. et al, 'Blast testing of ultra-high performance fibre and FRP-retrofitted concrete slabs', *Engineering structures*, vol 31, pp. 2060-2069, 2009.

[22] Yi n. et al., 'Blast-resistant characteristics of ultra-high strength concrete and reactive powder concrete', *Construction and Building Materials*, vol 28, pp. 694-707, 2012.

[23] Barnett S. et al., 'Ultra high performance fibre reinforced concrete for explosion resistant structures', *Proceedings of Concrete Platform*, Queen's University of Belfast, Belfast, UK, pp. 565-567, 2007.

[24] Mellen P., 'Blast and fragmentation loading indicative of a VBIED surrogate for structural panel response analysis', *International Journal of Impact Engineering,* vol 126, pp. 172-184, 2019.

[25] Sobuz H. et al., 'Manufacturing ultra-high performance concrete utilising conventional materials and production methods', *Construction and Building Materials*, vol 111, pp. 251-261, 2016.

[26] ConWep [software], United States Army Corps of Engineers Protective Design Center, Omaha, Nebraska, 2002.

[27] SBEDS_v5.1 [software], United States Army Corps of Engineers Protective Design Center, Omaha Nebraska, 2015.

[28] 'TM 5-1300 Structures to Resist the Effects of Accidental Explosions', US Army Corps of Engineers, Washington, USA, 1990.

[29] Nichols J. and Nelson J., The Current State of the Vulnerability Assessment and Protection Option (VAPO) Software Program and its Applicability to the Explosives Safety Community, Defense Threat Reduction Agency, Fort Belvoir Virginia, 2018

6. Summary and Conclusions

Summary

The main goal of this thesis was to improve understanding of how the blast and fragmentation loadings produced by VBIEDs load concrete panels. The two primary aims were:

1. To accurately measure the pressure and fragmentation loadings of a VBIED surrogate charge, and the pressure loading of a comparative bare charge, in the near field.
2. Investigate the deflection of structural panels, constructed from low and high technology materials, when subjected to the blast and fragmentation loadings produced by the VBIED surrogate and bare charges, and determine the significance of the VBIED fragmentation loadings.

Experiments were conducted, and data successfully collected to achieve both of these aims. A range of concrete panels constructed of low strength, moderate strength, and ultra-high-performance concrete were tested.

Conclusions

The following conclusions were ascertained from the work undertaken:

- Bare charge size was tuned to attempt to match the pressure and impulse output of the VBIED surrogate. Whilst both the pressure and impulse could not be simultaneously matched a sufficiently similar output was produced where a slightly higher peak pressure but lower impulse was generated. In future it would be more important to match the impulse than the peak pressure when considering panel response.
- Accurate histories were recorded for both incident pressures at various distances from the charge and reflected pressures across the target panel. These pressure histories were found to be highly consistent across a large number of tests. Clearing effects were observed in the reflected pressure histories, however they were relatively minor. The data for the pressure loadings was sufficiently consistent and accurate such that it can be used to reproduce these loadings in numerical simulations.
- Fragment distributions and speeds were recorded for the VBIED surrogate. Whilst considerably more consistent than a VBIED, substantial variation was recorded between tests. This was predominantly due to variation in the number of fragment impacts on the target panel area. The fastest fragment speeds averaged approximately 370 m/s. As the fragments had a mass of 92 g this resulted in an energy of 12 kJ per fragment.
- Test panels constructed of low strength, moderate strength, and ultra-high performance concrete were tested against both bare charges and the VBIED surrogate. The temporal response of the panels at the half and quarter heights was accurately recorded with two different forms of instrumentation. The results from both forms of instrumentation were in good agreement.
- The impulse produced by the VBIED surrogate fragment impacts was sufficient to generate a global response for all panels tested. Therefore, it is vital that the contribution of fragments is considered when estimating the structural response of panels to VBIED threats.

- The relationship between the flexural stiffness of the panel and the difference in time of arrival for the fragment and blast loads was found to be highly significant on the maximum deflection of the panels:
    - For panels with lower flexural stiffnesses the combined blast and fragmentation loadings produced sufficient damage to reduce the stiffnesses of the panels.
    - Synergistic loading effects were only significant for panels with a sufficiently low flexural stiffness.
- UHPC panels had lower deflections and shallower craters, than panels constructed of conventional concretes, when subjected to the loads produced by the bare charges and the VBIED surrogate charges. As such the material could be utilised to provide improved levels of protection against VBIED threats.

Future Work

The data recorded for the pressure loadings was sufficiently accurate and consistent so as to be used as an input in simulations. The fragmentation loadings produced by the VBIED surrogate still had a moderate variability in the trajectories of the preformed fragments, resulting in variation in the number of fragment impacts on the test panels. However, the fragment velocities were reasonably consistent. As such a very similar fragment loading could be produced in a simulation. Additionally, the recovered fragments showed very little deformation. As such, in simulations the model fragments could be reasonably modelled as unresponsive cuboids to assist in minimising computational strain.

These loads could be both reproduced in a simulation to produce a Virtual Laboratory in which new material models for structural panels could be tested. A large number of tests could be run in this Virtual Laboratory as no significant cost, with a small number of verification tests being undertaken on a test range in the same fashion as the tests described in this thesis. This would greatly reduce the cost in developing new material models.

The structural materials utilised in these tests could be modelled in a Virtual Laboratory to gauge the validity of representing these materials with various current material models. This would be of particular use for UHPC as there is considerable interest in utilising this material in strengthening structures against blast and fragmentation loadings from VBIEDs.

The deformations recorded in this series of experiments were relatively minor. A further series of experiments could be conducted with lower strength or thinner panels. This would provide additional data at larger deflections. Tests of this type were not conducted in this experimental series due to the risk of damaging instrumentation.

The charges were consistently placed at the same distance from the test panels. In future tests the stand-off could be varied to determine how the blast and fragmentation loadings vary. The pressure and fragment conditions measured experimentally could be used to estimate the loading conditions at other stand-offs however this extrapolation may rapidly become inaccurate at significantly different scaled distances.

This work has been based on utilisation of a VBIED surrogate which produces fragments of identical size with similar velocities. This is a simplification of the highly variable distribution of fragments

produced by a VBIED. An improved surrogate could be improved by aggregating the fragment distribution into a limited number of sizing bins and having preformed fragments indicative of each of these bins. Additionally, there are some ejecta that are notable but not distributed and may not be frequently referred to as fragments. An example of this is the engine block, which often is ejected reasonably intact. These ejecta could be independently considered as their slow velocities mean they would impact structural elements significantly later than the blast wave or smaller fragments.

The surrogate was designed to capture some aspects of the loadings produced by the VBIEDs tested in a previous experimental series. These VBIEDs did not capture the scale of variation in VBIED construction as all used similar sized vehicles and quantities of explosive material. Ideally further tests would be conducted with VBIEDs utilising various types of vehicles, ranging in size up to a box truck, and various amounts of explosive. This would improve understanding of the breadth of loading conditions that could be produced by VBIED threats.